

Inferring Properties of Graph Neural Network

THANH-DAT NGUYEN, University of Melbourne, Australia

MINH-HIEU VU, Independent Researcher, Vietnam

THANH LE-CONG, University of Melbourne, Australia

XUAN BACH D. LE, University of Melbourne, Australia

DAVID LO, Singapore Management University, Singapore

THANHVU NGUYEN, George Mason University, USA

CORINA PASAREANU, Carnegie Mellon University, USA

Graph Neural Networks (GNNs) are effective approaches for representing and analyzing many real-world graph-structured problems such as knowledge graph analysis, social networks recommendation, vaccine development and software analysis. Just like other types of neural networks such as feed-forward neural networks (FNNs) and convolutional neural networks (CNNs), the neural networks' robustness against attacks, e.g., backdoor attacks, remains an important concern. To address this problem, property inference techniques have been proposed for FNNs and CNNs. These techniques, however, are not applicable to GNNs since they assume fixed-size inputs, as opposed to input graphs of varying structures allowed by GNNs.

In this paper, we propose GNN-Infer, the first automatic property inference technique for GNNs. To tackle the challenge of varying input structures in GNNs, GNN-Infer first identifies a set of representative influential structures that contribute significantly towards the prediction of a GNN. Using these structures, GNN-Infer converts each pair of an influential structure and the GNN to their equivalent FNN and then leverages existing property inference techniques to effectively capture properties of the GNN that are specific to the influential structures. GNN-Infer then generalizes the captured properties to any input graphs that contain the influential structures. Finally, GNN-Infer improves the correctness of the inferred properties by building a model that estimates the deviation of GNN output from the inferred properties given full input graphs. The learned model helps GNN-Infer extend the inferred properties with constraints to the input and output of the GNN, obtaining stronger properties that hold on full input graphs.

Our experiments show that GNN-Infer is effective in inferring likely properties of popular real-world GNNs, and more importantly, these inferred properties help effectively defend against GNNs' backdoor attacks. In particular, out of the 13 ground truth properties, GNN-Infer re-discovered 8 correct properties and discovered likely correct properties that approximate the remaining 5 ground truth properties. Furthermore, on popular real-world GNNs, GNN-Infer inferred properties that can be used to effectively defend against the state-of-the-art backdoor attack technique on GNNs, namely UGBA. Experiments show that GNN-Infer's defense success rate is up to 30 times better than existing defense baselines.

Additional Key Words and Phrases: Graph neural networks, property inference, network conversion, neural network debugging

1 INTRODUCTION

Deep neural networks (DNNs) are widely recognized as state-of-the-art in tackling a wide range of problems such as natural language processing [37, 62], computer vision [27, 51], and software engineering [17, 39, 58]. Two primary types of DNNs are (i) networks that take fixed-size input, i.e., inputs that have predefined sizes, such as feed-forward neural networks (FNNs) and convolutional neural networks (CNNs) [15, 16, 26] and (ii) networks that take inputs with varying sizes and structures, such as graph neural networks (GNNs) [11, 25, 41, 65].

Authors' addresses: Thanh-Dat Nguyen, thanhdatn@student.unimelb.edu.au, University of Melbourne, Australia; Minh-Hieu Vu, Independent Researcher, Vietnam; Thanh Le-Cong, University of Melbourne, Australia; Xuan Bach D. Le, bach.le@unimelb.edu.au, University of Melbourne, Australia; David Lo, davidlo@smu.edu.sg, Singapore Management University, Singapore; ThanhVu Nguyen, tvn@gmu.edu, George Mason University, USA; Corina Pasareanu, pcorina@andrew.cmu.edu, Carnegie Mellon University, USA.

GNNs are a powerful tool for modeling complex data structures. Problems including detecting fake users [47], fake news [32], and performing recommendations [48, 59] on social media to mimicking classic combinatorial optimization [3, 50] and detecting faults in software [2, 36, 66] can be straightforwardly modeled using graphs. In these representations, a graph can have varying numbers of nodes and edges, for example, a person in social networks can have varying numbers of friends, or a molecule can have varying numbers of atoms, etc [67]. While CNNs and FNNs are not designed for such varying data structures, GNNs can naturally handle these varying structures using the message-passing mechanism [11]. However, the complexity of the message-passing mechanism renders it difficult to debug GNNs, e.g., assessing the robustness of GNNs against adversarial attacks [6, 30, 55, 68, 70] or detecting backdoor behaviors [5, 56, 63]. To tackle GNNs debugging, existing explainable AI techniques provide heatmaps to help human experts *manually* debug GNNs [18, 28, 60]. To the best of our knowledge, there does not exist any technique that supports automated debugging of GNNs.

There, however, exists recent works on automated debugging of CNNs and FNNs by inferring formal properties to interpret and assess deep neural network performance [10, 13, 44]. These techniques take as input a DNN along with a set of *fixed-size* and *fixed-structure* input data, and then infer a set of formal properties that are logical constraints that capture the relationships between the input and output of the DNN. Despite being powerful, these techniques cannot handle inputs with varying sizes and structures such as graphs wherein the number of nodes and edges, and the connections between them can dynamically change. It is thus significantly challenging to adopt these techniques for automated debugging of GNNs.

In this work, we introduce GNN-Infer, the first automatic property inference technique for GNNs to facilitate automated debugging of GNNs. GNN-Infer tackle the challenge of dynamic input graph structures in GNN in three steps, each of which is a novel contribution. First, we select a set of representative input structures to analyze. Second, we infer GNN’s properties on each of the representative structures. Finally, we generalize these properties to varying structures that contain the representative structures. To achieve these, GNN-Infer first mines the *most frequent influential* structures, which appear frequently in the dataset and contribute significantly towards GNN’s prediction. These structures are more likely to capture GNN’s behavior as shown in prior works [29, 61], and are thus considered representative input structures. Next, for each influential structure S as input to a GNN model \mathcal{M} , GNN-Infer converts the pair $\langle \mathcal{M}, S \rangle$ into an equivalent FNN model \mathcal{M}_F . We formally prove that our conversion algorithm is both sound, i.e., \mathcal{M}_F is indeed equivalent to $\langle \mathcal{M}, S \rangle$, and complete, i.e., given any $\langle \mathcal{M}, S \rangle$, there always exists an equivalent \mathcal{M}_F . This enables us to leverage an existing property inference technique for FNNs, namely PROPHECY [13], to infer a set of properties $\{S_P\}$. These inferred properties $\{S_P\}$ are then considered the properties of the original GNN \mathcal{M} on the given structure S .

Note that the inferred properties $\{S_P\}$ are still specific to the frequent influential structures: each property S_P imposes an input condition that the input graph must have the *exact* structure as S . GNN-Infer then generalizes these properties to any input graph that contains the influential structures by relaxing each S_P into a likely property S_{LP} , in which the imposed input condition is that the input graph must *contain* the structure S . When the imposed input condition is relaxed, the likely property S_{LP} might lose precision. GNN-Infer improves the precision of these likely properties by training a model (either a decision tree or linear regression) that estimates the deviation of the GNN output from the inferred properties on a given full input graph. The predictions of the model help GNN-Infer obtain more precise properties that hold on the full input graph.

We evaluate GNN-Infer’s correctness and applicability on both synthetic and popular real-world datasets. To assess GNN-Infer’s correctness, we construct a synthetic benchmark consisting of reference GNN and corresponding ground truth properties: the constructed benchmark consists

of reference and trained GNNs to mimic classic breadth-first search (BFS) and depth-first search (DFS) and Bellman-Ford (B-F) algorithms. Manual assessments show that out of 13 ground-truth properties, GNN-Infer re-discovered 8 correct properties and identified highly confident properties that approximate the remaining ground-truth properties. As an application of GNN-Infer, we use its inferred properties to detect and defend against the state-of-the-art backdoor attack technique on GNNs, namely UGBA [5]. Experiments show that GNN-Infer’s inferred properties can be used to improve the defense against the state-of-the-art backdoor attack method UGBA [5] by up to 30 times in comparison with existing baseline defense methods [5]. In summary, we make the following contributions:

- We propose GNN-Infer which automatically infers properties of GNNs by analyzing and generalizing GNNs’ behaviors on representative structures.
- We provide an algorithm that converts a GNN with a given input structure to an equivalent FNN. We formally prove that the algorithm is both sound and complete, enabling us to use existing DNN analysis tools to infer properties of the GNN.
- We construct a set of benchmarks containing GNNs on classic traversal and shortest path algorithms to evaluate GNN-Infer and show that GNN-Infer can infer correct properties.
- Finally, we show that GNN-Infer can be used to improve the backdoor defense against state-of-the-art backdoor attack techniques on graph neural networks by up to 30 times in comparison with existing techniques, namely homophily-based pruning and isolation [5].

2 BACKGROUND

The key idea of GNN-Infer is based on transforming a GNN into an FNN. We now give a brief description of FNN and GNN.

Feed-forward Neural Networks [45]. Definition 1 and Definition 2 below give a formal definition of Feed-forward Neural networks.

DEFINITION 1. *A feed-forward layer is a function between m input variables x_1, \dots, x_m and n output variables y_1, \dots, y_n . This function is one of the following:*

- (1) *an affine transformation: $(y_1, \dots, y_n)^T = \mathbf{A}(x_1, \dots, x_m)^T + \mathbf{b}$.*
- (2) *the ReLU activation function $(y_1, \dots, y_n)^T = (\max(0, x_1) \dots \max(0, x_m))^T$. Note that for ReLU the number of input and output variables has to be the same (i.e., $m = n$).*
- (3) *a max pooling function, $(y_1, \dots, y_n)^T = (\max_{x \in P_1}(x), \max_{x \in P_2}(x), \dots, \max_{x \in P_n}(x))^T$ where P_1, \dots, P_n are predefined subsets of the input variable set $\{x_1, \dots, x_m\}$.*

DEFINITION 2. (FNN) *An l -layered FNN is a composition of l feed-forward layers.*

Intuitively, an FNN is a composition of specific operations applied to the input. The input of FNN is a vector $\mathbf{x} = [x_1, \dots, x_m]^T \in \mathbb{R}^m$ where m is the chosen dimension for input. Given this input, the applied operations are either linear affine transformations or non-linear activation functions. The output of FNN is the output vector $\mathbf{y} = [y_1, \dots, y_n]^T \in \mathbb{R}^n$, where n is the chosen dimension for output (i.e., number of classes in a classification problem).

Graph Neural Network [11]. Graph Neural Networks (GNNs), on the other hand, are a more recent development in the field of neural networks that focus on graph-structured data. They take as input a graph G , where each node and edge can be associated with their respective feature vector and make predictions on the graph, nodes or edges’ properties. Similarly to FNN, GNN (see Definition 4) is a composition of message passing layers defined in Definition 3.

DEFINITION 3. (Message Passing Layer) *A graph neural network layer is a function that takes as input a graph $G = (V, E)$, where V is the set of nodes and E is the set of edges, along with associated node feature \mathbf{x}_i for each node i and edge feature \mathbf{e}_{ji} for each edge $(j, i) \in E$, and return the updated node*

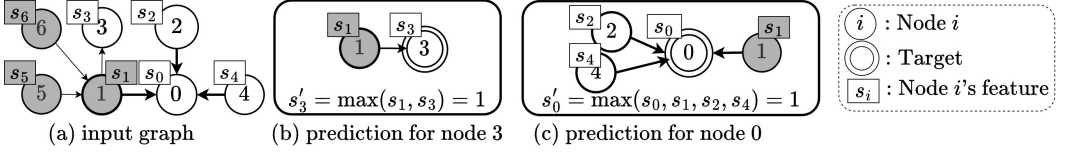


Fig. 1. Message passing process of BFS. While the GNN makes predictions in parallel for all nodes, we separate nodes 0 and 3's predictions for illustration shown in (b) and (c).

features \mathbf{x}'_i for each node $i \in V$. The update is based on the node's previous state and the aggregated states of its neighboring vertices and edges. Formally, the update rule for a node i can be defined as:

$$\mathbf{x}'_i = f_{upd}(\mathbf{x}_i, f_{agg}(\{f_{msg}(\mathbf{x}_j, \mathbf{x}_i, \mathbf{e}_{ji}) \mid (j, i) \in E\}))$$

where f_{agg} is an aggregation function, and f_{upd} is an update function and f_{msg} is a message passing function. f_{upd} and f_{msg} are FNNs according to Definition 2 and f_{agg} is either a linear combination or max aggregation over a set of vectors.

DEFINITION 4. A Graph Neural Network (GNN) is a neural network that operates on the graph domain and consists of a sequence of graph neural network layers. Each layer updates the vertices' states based on the graph structure and vertex and edge features. An l -layered GNN is a composition of l such layers, with the output of each layer serving as the input to the next layer.

A GNN takes as input a graph $G = (V, E)$ with associated node features \mathbf{x}_i for each node $i \in V$, and edge features \mathbf{e}_{ji} for each edge $(j, i) \in E$ where V is the node set and E is the set of edges, where each node and edge is associated with their own feature vectors. The GNN iteratively computes new features for nodes via message-passing layers. Each message passing layer first calculates the message $m_{j,i}$ for each edge $(j, i) \in E$ by making use of the message passing function f_{msg} . Following that, the aggregation function f_{agg} comprises the incoming messages (i.e., vectors) for each individual node i into an aggregated message (a single vector). Finally, this aggregated message is transformed by another update function f_{upd} , resulting in the updated node features.

As an example, we take a GNN simulating Breadth-first search (BFS) algorithm in (Fig 1), following [50]. This GNN takes as input a graph, where each node i is associated with a single feature $s_i \in \{0, 1\}$ denoting whether the node has been visited (1) or not (0), and predicts these nodes' visiting state in the next step. Let the message and update functions be an identity function (i.e., $f(x) = x$), the aggregation is chosen as the max aggregation. With this combination, each individual node's update features will be calculated as $s'_i = \max\{s_j \mid (j, i) \in E\}$, meaning that each node's new features is the maximum among its neighbors features. To see how this GNN works, let us take as input a graph with 7 nodes in Fig 1. nodes 3, receiving incoming edges from node 1 and node 0, receiving incoming edges from nodes 1, 2, 4, are predicted as *visited* (Fig. 1) since node 1, among their neighbor is visited. In practice, this message-passing mechanism allows GNN to handle arbitrary input graphs, of which sizes and structures directly affect the computation. Due to the complexity of the message-passing mechanism, there does not exist formal techniques and tools for analyzing GNNs.

Our GNN-Infer approach aims to reduce a GNN to an FNN, and take advantage of existing FNN analyses to infer properties for GNNs. Note that for illustration, the above example gives a very simple message-passing procedure that is just identity functions. Our approach GNN-Infer indeed supports even more complicated message-passing procedures, e.g., f_{msg} and f_{upd} can be FNNs

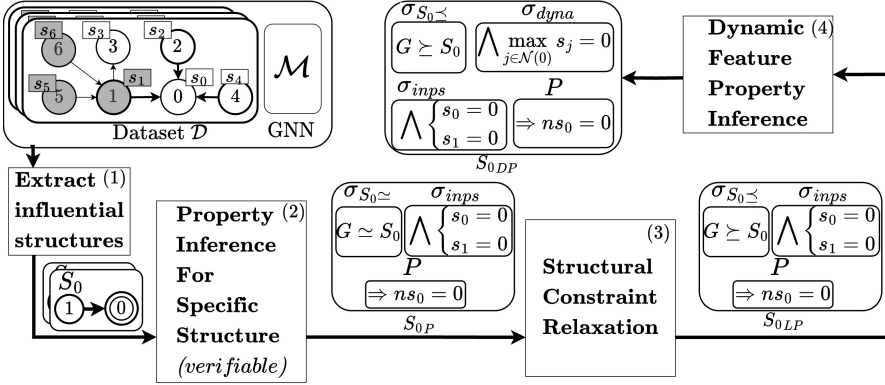


Fig. 2. GNN-Infer Overview.

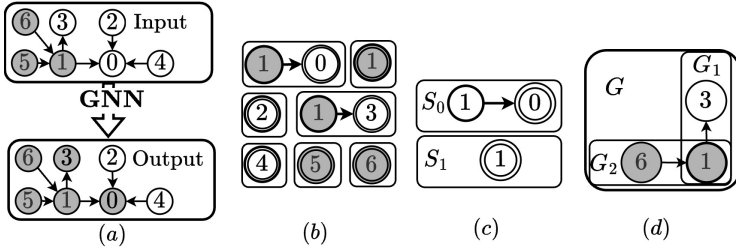


Fig. 3. (a) a GNN step, visited nodes are grey-colored (b) Example of influential structure for each node for the GNN step, where each influential structure contributes significantly to the target node denoted in the double circles. (c) the most frequented influential structures and (d) graph matching of between S_0 and G .

themselves and can operate on a heterogeneous graph similar to those in the literature [42, 64]. In Section 3, we give an overview of GNN-Infer and how it works on the BFS example in Fig. 1.

3 OVERVIEW AND MOTIVATING EXAMPLE

Fig. 2 presents an overview of GNN-Infer, which takes as inputs a trained GNN model \mathcal{M} and a dataset \mathcal{D} , and outputs likely GNN properties and structure-specific properties. GNN-Infer comprises four stages: (i) extracting influential substructures, (ii) inferring properties for specific structures, (iii) relaxing structure constraints, and (iv) inferring dynamic feature properties. Below, we explain these steps and also how it works on the BFS example presented in Fig. 1.

Extract influential structures. This step analyzes the model \mathcal{M} and dataset \mathcal{D} to compute influential structures, which are subgraphs that frequently appear in the dataset and significantly impact GNN predictions. GNN-Infer identifies influential structures for individual nodes using GNNExplainer [60] and gSpan [57]. For example, in the BFS GNN prediction of Fig. 3a, GNN-Infer first detects influential structures for each node. In this case, the influential structure for node 0 is a subgraph containing node 1 and node 0 with an edge from node 1 to 0, because node 0 is predicted as visited due to its connection with the visited node 1. For node 1, its influential structure is just itself, since it would remain to be visited regardless of its neighbors' states. The result of applying

this process to all nodes is illustrated in Fig. 3b. Then, from these influential structures of all nodes, GNN-Infer chooses the two most frequently appeared structures S_0 and S_1 in Fig. 3c.

Property inference for specific structure. For each influential structure S , GNN-Infer infers a set of structure-specific properties $\{S_P\}$, each in the form of $\sigma_{S \simeq} \wedge \sigma_{inps} \Rightarrow P$. $\sigma_{S \simeq}$ is a structure condition requiring the input graph to be isomorphic with S , σ_{inps} is an input feature condition, and P is an output condition on prediction values. GNN-Infer uses Neo4J [34] to collect all graph matching the structure condition $\sigma_{S \simeq}$ from the dataset \mathcal{D} , transforms the GNN model \mathcal{M} and structure S into an equivalent model \mathcal{M}_F , and employs PROPHECY [13] to identify σ_{inps} and P .

For the BFS example, GNN-Infer derives properties for substructure S_0 for node 0 like $\sigma_{S_0 \simeq} \wedge s_0 = 0 \wedge s_1 = 0 \Rightarrow s'_0 = 0$ and $\sigma_{S_0 \simeq} \wedge s_0 = 1 \Rightarrow s'_0 = 1$. These indicate that for input graphs isomorphic with S_0 (containing edge $1 \rightarrow 0$), the GNN predicts node 0 is unvisited if both node 1 and itself are unvisited, and visited if node 1 is visited. For substructure S_1 , GNN-Infer obtains a property stating that for input graphs isomorphic with S_1 , node 1’s predicted status equals its current status.

The found properties apply only to graphs isomorphic with influential substructures, enabling GNN-Infer to use automatic verification like Marabou [23]. However, these structure-specific properties are limited (e.g., only applicable to the graphs with this exact structure).

Structure Constraint Relaxation. GNN-Infer generalizes each structure-specific property to a *subgraph isomorphic* property, covering a broader set of input graphs. We obtain properties like $\sigma_{S \leq} \wedge \sigma_{inps} \Rightarrow P$, where $\sigma_{S \leq}$ denotes subgraph isomorphism condition (i.e., input graph has to contain structure S). In the BFS example, GNN-Infer derives $\sigma_{S_0 \leq} \wedge s_i = 0 \wedge s_j = 0 \Rightarrow s'_i = 0$, which means that any input graph that *contain* this structure S_0 , with both node i and j (neighbor of node i) being unvisited, then the new state of node i will also be *unvisited*. These isomorphic properties are more general and useful but, as they cover dynamic structures, GNN-to-FNN conversion and verification using existing DNN tools are not possible, making them likely properties.

Dynamic Property Inference. To enhance the precision of likely properties, GNN-Infer augments them with dynamic feature properties, capturing output postcondition changes relative to an aggregated feature set of the GNN. To do this, GNN-Infer computes feature formulae from the trained GNN, collects feature values for input graphs in dataset \mathcal{D} , and trains a decision tree or linear regression on them. For classification problems, GNN-Infer predicts whether condition P holds on the full graph and constructs dynamic feature predicate σ_{dyna} using tree paths leading to $P = True$. The dynamic property is $\sigma_{S \leq} \wedge \sigma_{inps} \wedge \sigma_{dyna} \Rightarrow P$. For regression problems, GNN-Infer trains a linear regression model to capture deviation between condition P and GNN’s actual output, obtaining new output condition P_{dyna} and dynamic property $\sigma_{S \leq} \wedge \sigma_{inps} \Rightarrow P_{dyna}$.

Using the BFS example, GNN-Infer extracts the dynamic feature $\max_{j \in \mathcal{N}(i)} s_j$ for nodes in structure S . This feature incorporates surrounding node information. GNN-Infer collects aggregated feature values and builds a decision tree to predict property applicability. The logical formula is combined with the structure-property to obtain the full property, ensuring accurate predictions. If the property already matches all instances in the dataset, no dynamic condition is added.

Finally, the results of GNN-Infer are likely properties in either the form of $\sigma_{S \leq} \wedge \sigma_{inps} \wedge \sigma_{dyna} \Rightarrow P$ for classification problems or $\sigma_{S \leq} \wedge \sigma_{inps} \Rightarrow P_{dyna}$ for regression problems. These properties show that if the input graph containing the structure S , having input features matching σ_{inps} and σ_{dyna} , then the output property (P or P_{dyna}) is implied. These properties show specific behaviors of the GNN on a class of graphs and can be used for precise analysis of GNN, one example is using these properties to find backdoor behaviors and prune the backdoored graph (See Section 5.3)

4 THE GNN-INFER APPROACH

We now present in more details of our approach GNN-Infer illustrated in Fig. 4. GNN-Infer takes a trained GNN model \mathcal{M} and dataset \mathcal{D} as inputs. First, we extract influential structures $\{S\}$ given

Input : A trained GNN model \mathcal{M} , training dataset \mathcal{D}
Output: A set of structure-specific properties SP , and a set of dynamic feature properties DP

```

1  $IS \leftarrow \text{ExtractStructures}(\mathcal{M}, \mathcal{D})$ 
2  $SP \leftarrow \{\}, DP \leftarrow \{\}$ 
3 foreach  $structure\ S \in IS$  do
4      $\sigma_{S \simeq} \leftarrow \text{ConstructGraphIsomorphicPredicate}(S)$ 
5      $\sigma_{S \leq} \leftarrow \text{ConstructSubgraphIsomorphicPredicate}(S)$ 
6      $\{S_P\} \leftarrow \text{InferStructSpecificProps}(\sigma_{S \simeq}, \mathcal{M}, \mathcal{D})$ 
7     foreach  $S_P \in \{S_P\}$  do
8          $SP.add(S_P)$ 
9          $S_{LP} \leftarrow \text{RelaxConstraint}(S_P, \sigma_{S \leq})$ 
10         $S_{DP} \leftarrow \text{DynamicAnalysis}(S_{LP}, \mathcal{M}, \mathcal{D})$ 
11         $DP.add(S_{DP})$ 
12 return  $SP, DP$ 
    
```

Fig. 4. The GNN-Infer approach

the model \mathcal{M} and dataset \mathcal{D} . Followed by that, we convert each $\langle \mathcal{M}, S \rangle$ to an equivalent FNN \mathcal{M}_F , collecting \mathcal{M}_F 's execution trace given dataset \mathcal{D} and inferring structure-specific properties $\{S_P\}$ given the obtained execution traces. Finally both \mathcal{M} and \mathcal{D} are used to generalize each structure-specific property $\{S_P\}$. Note that GNN-Infer works on any \mathcal{D} that are graphs, and we show in Section 5 that GNN-Infer works well on existing popular dataset and GNN models. Next subsections explain each step of GNN-Infer in details.

4.1 Extracting Influential Substructures

The use of *most frequent influential structures* empowers GNN-Infer to more efficiently and effectively analyze a GNN. Our intuition is that: (1) The frequent influential structures are smaller than full graphs, rendering them more efficient to analyze. (2) They contribute significantly to the GNN's prediction, and hence, they help reveal common behaviors of the GNN. Towards this end, GNN-Infer uses GNNExplainer [61] to identify the influential structures and Subdue [24] to find the most frequent structures among the set of all influential structures.

While the GNN makes predictions for all nodes of the input graph in parallel, each node's prediction can be influenced by different parts of the input graph as shown in Fig. 3 and Section. 3. To precisely capture the influential structures of the GNN, we identify the influential structure for each node prediction individually. The chosen node is called the *target* node. This is done by applying GNNExplainer [61] on the target node prediction. The GNNExplainer takes as input a graph, the model \mathcal{M} , and the target prediction and outputs important scores for each node and edge in the input graph towards the prediction. We retrieve the influential structure from the important score by keeping the nodes and edges having sufficient important scores (above the threshold of 0.8 in our implementation). Retrieving each node's influential structure would give us a set of *influential structures* IS in the dataset \mathcal{D} with respect to the model \mathcal{M} . On this set IS , we apply gSpan [57] to obtain a small set of *frequent influential structures*.

Example. Taking the example in Fig. 3, each node 0, 1, 2, 3, 4, 5, 6 has a distinct influential structure. Each of these influential structures is associated with a target node and contains information on the set of nodes, edges, node types, and edge types (without node or edge features). These structures are smaller than the input graph (e.g., node 0's influential structure consists of only two nodes and one edge in comparison with 7 nodes and 6 edges of the original input graph). Performing frequented

subgraph mining would give us 2 most frequented influential structures: (1) The structure has a single node and (2) the structure has two nodes (e.g., node 0’s influential structure). This set of frequent influential structures is used in a later step as structure predicates described in Section 4.2, which are used to govern the constraint over which graph structures to be analyzed.

4.2 Structure Predicates

Structure predicates are used to describe the constraints over which graph structures that GNN-Infer focuses on analyzing. Below, we provide a formal definition of structure predicates.

Recall that a GNN takes as input a graph $G = (V_G, E_G)$. Each influential structure $S = \langle V_S, E_S \rangle$ is a subgraph of G , and is influential towards a single prediction. Since GNN-Infer performs properties inference for specific structures, and subsequently generalizes the input for the structures that contain these specific structures, we use isomorphism and subgraph isomorphism as structure predicates.

Intuitively, given a graph G' , an isomorphism predicate on a graph G checks whether G' and G has identical structure. We define graph isomorphic as \simeq and the G' -isomorphic predicate as $\sigma_{G' \simeq}$ as follows:

$$\sigma_{G' \simeq}(G) := G' \simeq G := \exists h : V_G \rightarrow V_{G'} \text{ s.t. } \begin{cases} \forall i \in V_G, i \in V_{G'} \\ \forall i, j \in E_G, (h(i), h(j)) \in E_{G'} \text{ and} \\ \forall (i, j) \notin E_G, (h(i), h(j)) \notin E_{G'} \end{cases} \quad (1)$$

This indicates that there must exist a bijective mapping between the nodes of G and G' such that if a node or an edge exists in G , it must have the corresponding node or edge in G' and vice versa. This isomorphic condition is strict and requires that there exists no redundant edge in G (i.e., G and G' have to be identical in term of structure). We use this as a structure predicate for the structure-specific properties.

Additionally, if a graph G contains a subgraph that is isomorphic to G' , this would result in subgraph-isomorphic condition \leq . Specifically, let us also define the subgraph isomorphic operation as \leq and the G' -subgraph isomorphic predicate $\sigma_{G' \leq}$ as follows:

$$\sigma_{G' \leq}(G) := G' \leq G := \exists h : V_{G'} \rightarrow V_G \text{ s.t. } \begin{cases} \forall i \in V_{G'} : h(i) \in V_G \\ \forall i, j \in E_{G'}, (h(i), h(j)) \in E_G \end{cases} \quad (2)$$

This definition specifies that there exists an injective function h from the node set of G' to the node set of G such that every edge G' corresponds to an edge in G , thus ensuring that the mapped vertices from G form a subgraph isomorphic to G' . Intuitively, this can be understood as a more relaxed version of graph isomorphic condition.

Structure predicates are then formally defined as:

$$\sigma_{struct} := \begin{cases} \sigma_{S \simeq} & \text{When using graph-isomorphic constraint} \\ \sigma_{S \leq} & \text{When using subgraph-isomorphic constraint} \end{cases} \quad (3)$$

Example. Consider the structure S_0 illustrated in Fig. 3. We define $S_0 = \{\{0, 1\}, \{(1, 0)\}\}$, having 2 nodes 0, 1 and one edge from 1 to 0 and S_0 is influential towards the prediction of target node 0. $\sigma_{S_0 \simeq}(G)$ and $\sigma_{S_0 \leq}(G)$. In this example, graph G is not isomorphic towards S_0 . But G contains two subgraphs G_1 and G_2 that is isomorphic towards S_0 . Hence, $\sigma_{S_0 \simeq}(G_1) = True$ and $\sigma_{S_0 \simeq}(G_2) = True$. Moreover, $G_1, G_2,$ and G are all subgraph-isomorphic towards S_0 , thus, $\sigma_{S_0 \leq}(G_1) = \sigma_{S_0 \leq}(G_2) = \sigma_{S_0 \leq}(G) = True$.

4.3 Property Inference for Specific Structure

This step takes the GNN \mathcal{M} , the dataset \mathcal{D} , a structure S and outputs a set of structure-specific properties $\{S_P\}$. Each structure specific property S_P have the form of $\sigma_{S \simeq} \wedge \sigma_{inps} \Rightarrow P$. Here, $\sigma_{S \simeq}$

specifies graph-isomorphic predicate in Section 4.2, while σ_{inps} is the input feature predicate, and P is the output property. The input feature predicate σ_{inps} specifies a set of linear inequalities on the input features of each node \mathbf{x}_i and each edges \mathbf{e}_{ji} , while the output property P either specifies a chosen output class of each node for classification problems or a linear relation between the output and the input for regression problems.

To achieve the above, GNN-Infer first transforms the pair $\langle \mathcal{M}, S \rangle$ into a corresponding FNN \mathcal{M}_F . We prove that this transformation is both sound and complete (See Section 4.3.1). Based on this theoretical foundation, we then use PROPHECY [13], a property inference tool for FNN, to infer the properties of \mathcal{M}_F . The inferred properties are then considered to be properties of the original GNN \mathcal{M} .

Note that the inferred properties are specific to the input structure S . Since PROPHECY's inferred properties are guaranteed to be correct (verified by the Marabou tool [23] used in PROPHECY), these properties are correct on the original GNN when the input graph is isomorphic with S .

4.3.1 Theory and proof of transformation from GNNs to FNNs. This section demonstrates a sketch proof that, for any given Graph Neural Network (GNN) model \mathcal{M} following Definition 4, and an input structure $S = (V_S, E_S)$, the pair $\langle \mathcal{M}, S \rangle$ is reducible to an equivalent FNN \mathcal{M}_F .

We start the proof by introducing two lemmas to show that (1) the composition of different neural networks is a neural network (2) and also, the layer-wise combination of different l -layer neural networks is a l -layer neural network. In the context of our work, we define a layer-wise combination of different l -layer FNNs in Definition 5 below.

DEFINITION 5. (*Layer-wise combination of FNNs*) Given a set of l -layered FNNs $\{\mathcal{M}_{F_1}, \mathcal{M}_{F_2}, \dots, \mathcal{M}_{F_n}\}$, each \mathcal{M}_{F_i} defines a relation between its input and output variables, a layer-wise combination of $\{\mathcal{M}_{F_1}, \dots, \mathcal{M}_{F_n}\}$ is a composition of l relations $L^{(1)}, \dots, L^{(l)}$, where each relation $L^{(i)}$ is formed by combining each i th layer of all the models $\mathcal{M}_{F_1}, \dots, \mathcal{M}_{F_n}$: $L^{(i)}$'s input and output variable sets are unions of the input and output variable sets of all layers forming it respectively and the relation between these input and output variable sets is defined FNNs' layers.

This composition is common in FNN, demonstrating the process in which the results of each layer can be concatenated, added in different FNN architectures to form the final results. We also show that every layer-wise combination of an FNN results in an FNN itself in Lemma 1 below.

LEMMA 1. *The layer-wise combination of n l -layered FNNs $\mathcal{M}_1, \dots, \mathcal{M}_n$ is a FNN.*

Each layer's combination produces a new layer that computes relations depending on the combination of the input and output variable sets of the corresponding layers from the original FNNs. Furthermore, we can show that the composition of multiple FNNs also result in another FNN according to Lemma 2.

LEMMA 2. *The composition of k Feed-forward Neural Network $\mathcal{M}_1, \dots, \mathcal{M}_k$, where $\mathcal{M}_i : \mathbb{R}^{n_i} \rightarrow \mathbb{R}^{n_{i+1}}$, is a Feed-forward Neural Network.*

This establishes the basis for combining different neural network layers while preserving the FNN structure. Lemma 2 affirms that the composition of k FNNs results in another FNN. Next, we show that, given a fixed structure as input to a GNN, every layer of the GNN is reducible to a FNN:

LEMMA 3. *Given a graph G with fixed structure (i.e., the edge set E remains unchanged), and the hidden features $\mathbf{x}_i \in \mathbb{R}^D$ is produced by a feed-forward neural network in Definition 2, a graph neural network's message passing layer as defined in Definition 3 is reducible to a feedforward neural networks defined by Definition 2.*

This lemma provides a critical reduction, indicating that a layer in a GNN, even when the graph structure is fixed, can be considered analogous to a layer in an FNN. Given that GNNs operate on graph structures and FNNs on flat inputs, this bridges the gap by showing that the graph-based message-passing procedure can be reformulated as FNN operations. Finally, we establish Theorem 1:

THEOREM 1. *When given a structure S , prediction of a GNN \mathcal{M} defined by Definition 4 on S is reducible to a FNN \mathcal{M}_F as defined in definition 2.*

Theorem 1 says that every pair of a GNN model \mathcal{M} and any arbitrary input structure S is reducible to an equivalent FNN \mathcal{M}_F . The full proof for this theorem is available in Appendix B. Intuitively, GNN-Infer converts f_{msg} , f_{agg} , and f_{upd} for each layer sequentially into an equivalent FNN. Since each layer is applied to the input in a compositional manner, this conversion results in an FNN following Lemma 2.

4.3.2 Transformation algorithm based on Theorem 1. Using the recursive transformation in the proof above, we design the GNN-to-FNN transformation algorithm in Fig. 5. Following Theorem 1, the algorithm is proved to be both sound, i.e., the converted FNN \mathcal{M}_F is equivalent to $\langle \mathcal{M}, S \rangle$ and complete, i.e., every GNN model \mathcal{M} , given a fixed structure S , is convertible into an FNN \mathcal{M}_F .

Input: Graph Neural Network \mathcal{M} with k layers, Structure S
Output: Equivalent Feed-forward Neural Network \mathcal{M}_F

- 1 $\mathcal{M}_F \leftarrow$ an empty Feed-forward Neural Network
- 2 **for** $i \leftarrow 1$ **to** k **do**
- 3 Extract the i -th layer of GNN \mathcal{M} , denoted as L_i
- 4 Determine the corresponding FNN layer F_i based on the type of f_{agg} used in L_i
- 5 **foreach** node $j \in V_S$ **do**
- 6 $\mathcal{N}(j) \leftarrow \{j' \in V_S \mid (j', i) \in E_S\}$
- 7 **if** f_{agg} is mean aggregation **then**
- 8 $F_{i,j} := f_{upd} \left(\frac{1}{|\mathcal{N}(j)|} \mathbf{1}_{|\mathcal{N}(j)|}^\top \left\| \left\|_{k \in \mathcal{N}(j)} f_{msg}(\mathbf{x}_k^{(i)}, \mathbf{x}_j^{(i)}, \mathbf{e}_{kj}) \right\| \right) \right)$
- 9 **else if** f_{agg} is max aggregation **then**
- 10 $F_{i,j} := f_{upd} \left(\max_{k \in \mathcal{N}(j)} f_{msg}(\mathbf{x}_k^{(i)}, \mathbf{x}_j^{(i)}, \mathbf{e}_{kj}) \right)$
- 11 **else if** f_{agg} is sum aggregation **then**
- 12 $F_{i,j} := f_{upd} \left(\mathbf{1}_{|\mathcal{N}(j)|}^\top \left\| \left\|_{k \in \mathcal{N}(j)} f_{msg}(\mathbf{x}_k^{(i)}, \mathbf{x}_j^{(i)}, \mathbf{e}_{kj}) \right\| \right) \right)$
- 13 Append F_i to \mathcal{M}_F

Fig. 5. Reduction of a Graph Neural Network to a Feed-forward Neural Network. $\mathbf{x}_k^{(i)}$ denote the hidden features of node k at layer i (the output of the previously converted layer), $\left\| \left\| \right\|$ denotes the stacking operation which stacks each vector $\mathbf{x}_k \in \mathbb{R}^D$ to a form a matrix $\mathbf{X} \in \mathbb{R}^{N \times D}$ where N is the number of stacked vectors. $\mathbf{1}_{|\mathcal{N}(j)|}$ denote the all-1 vector with $\mathcal{N}(j)$ elements.

The goal of the transformation algorithm in Fig. 5 is to convert each individual message passing layer into the corresponding FNN, using them to construct the equivalent FNN that takes only node and edge features as input with no further concern on the structure. Since E_S is fixed, $\mathcal{N}(j)$ is also fixed for all $j \in V_S$, therefore, the final FNN \mathcal{M}_F only takes as input each node and edge's features. For more details, see Appendix C.

Example. Using S_0 in Fig. 3c and the GNN in the BFS example 1. In this case, the next state function is calculated as below for the target node:

$$S' = \mathbf{X}^{(1)} = \bar{\mathbf{M}} = \begin{pmatrix} \max(s_0, s_1) \\ s_1 \end{pmatrix} \quad (4)$$

The calculation of S' is an FNN \mathcal{M}_F based purely on the input feature instead of relying on the structure information. Given this equivalent FNN \mathcal{M}_F , we can now leverage PROPHECY to infer structure-specific properties.

4.3.3 Inferring Properties on FNN. Given the FNN \mathcal{M}_F transformed from a GNN \mathcal{M} and a structure S , we can now infer structure-specific properties using PROPHECY. PROPHECY requires as input *real* execution traces obtained by running the FNN on the training dataset. As a result, we need to collect all instances of the structure S from the original dataset and perform instrumentation on the FNN \mathcal{M}_F to gather its activation patterns and output.

To achieve the above, we make use of Neo4j [34] database. By encoding the full dataset as Neo4j graphs, we can efficiently retrieve instances of S through graph queries. Since \mathcal{M}_F is constructed from the original GNN through Algorithm 5, we automatically add instrumentation on non-linear layers during this transformation for actual instrumentation. Particularly, the instrumented points are (1) selected input variables in the max operation, (2) the activation of ReLU, and (3) conditions on the output. Having retrieved all the structure S 's instances in the dataset and added instrumentation, we collect the execution traces by running \mathcal{M}_F with all retrieved instances. With these instrumented execution traces, we use PROPHECY to infer the input constraints σ_{inps} that imply each output property P .

Example. Consider the converted network based on S_0 with the target node 0. Activation patterns are collected at the calculation of $\max(s_0, s_1)$: we record whether s_0 or s_1 is chosen in this operation for each instance of S_0 . If s_0 is chosen over node s_1 , then a condition on the input is $s_0 \geq s_1$ and vice versa. Additionally, output properties on the target node are collected, such as whether $s'_0 = 1$ or $s'_0 = 0$ for each execution. Using the FNN \mathcal{M}_F , activation patterns, and output properties, PROPHECY can infer input properties such as $s_0 = 1 \Rightarrow s'_0 = 1$, $s_1 = 1 \Rightarrow s'_0 = 1$, and $s_0 = 0 \wedge s_1 = 0 \Rightarrow s'_0 = 0$. Given $S_0 = \langle \{0, 1\}, \{(1, 0)\} \rangle$, the structure predicate $\sigma_{S_0 \simeq}$ is added to obtain structure-specific properties: $\sigma_{S_0 \simeq} \wedge s_0 = 1 \Rightarrow s'_0 = 1$, $\sigma_{S_0 \simeq} \wedge s_1 = 1 \Rightarrow s'_0 = 1$, and $\sigma_{S_0 \simeq} \wedge s_0 = 0 \wedge s_1 = 0 \Rightarrow s'_0 = 0$. It is worth noting that in practice, larger networks can result in more complex constraints over the input features.

4.4 Structure Condition Relaxation

While structure-specific properties are verifiable, their coverage is limited to a single structure. To increase the coverage of a property, we relax the structural constraint from $\sigma_{S \simeq}$ into $\sigma_{S \leq}$. This means that the input graph structure only has to *contain* (being subgraph isomorphic $\sigma_{S \leq}$) instead of being *equivalent* (isomorphic $\sigma_{S \simeq}$) to the structure S . Given a structure-specific property S_P in the form of $\sigma_{S \simeq} \wedge \sigma_{inps} \Rightarrow P$, the corresponding relaxed property S_{LP} is $\sigma_{S \leq} \wedge \sigma_{inps} \Rightarrow P$. Since this relaxation would allow the input graph to have varying numbers of nodes and edges again, the GNN computation can no longer be convertible into an FNN. Thus, the likely property S_{LP} can still be incorrect when the surrounding structure of the input graph changes.

Example. Taking the structure specific property $\sigma_{S_0 \simeq} \wedge s_0 = 0 \wedge s_1 = 0 \Rightarrow s'_0 = 0$ as input, the likely property is $\sigma_{S_0 \leq} \wedge s_0 = 0 \wedge s_1 = 0 \Rightarrow s'_0 = 0$. This resulting likely property can be imprecise. In detail, for the input graph in the example of Fig. 3a which contains 7 nodes, one S_0 's instance which matches this property is the subgraph containing two nodes 2 and 0 and one edge from 2 to

0. While $s_2 = 0$ and $s_0 = 0$, in this graph, $s'_0 = 1$ instead, this is because of node 0 has a neighbor 1 that is already visited. To improve the precision of likely properties, GNN-Infer perform dynamic feature property inference in Section. 4.5.

4.5 Dynamic Property Inference

S_{LP} might lose precision due to relaxed structure constraints specifying that the matching graphs only needs to *contain* the original structure S . Thus, the matching graphs can also contain additional nodes and edge features that were not originally included in the analysis of S and can influence the prediction of \mathcal{M} . The goal of this step is to improve the precision of S_{LP} with respect to these unaccounted nodes and edges' features. We do this by either adding the dynamic input feature predicate σ_{dyna} to S_{LP} or replacing the output property P in S_{LP} with a more precise dynamic output feature property P_{dyna} . Both σ_{dyna} and P_{dyna} are inferred by leveraging dynamic analysis over a set of aggregated features that take into account the surrounding features of S 's instances in the full graph.

Aggregated Features. To incorporate the full graph information, we compute the aggregated feature automatically using the GNN's first message-passing layer, which has several advantages in our settings. Firstly, towards the goal of incorporating surrounding information when analyzing GNN, using its own message-passing layer is a straightforward solution. Secondly, since we also want the inferred properties to be lightweight and interpretable, using the first message-passing layer allows the features to have an interpretable format, as we shall show in the example below.

GNN-Infer calculates three sets of aggregated features for each node i in the influential structure. The first set is structural aggregated features \mathbf{x}_i^{in} , using only the influential structure. The second set is full-graph aggregated features \mathbf{x}_i^{full} , using the full input graph. Finally, the third set is the subtraction $\mathbf{x}_i^{full} - \mathbf{x}_i^{in}$, allowing a simple comparison between the structural features and full structure features. Note that, if multiple message passings on different types of edges are employed, there will be multiple structural features and full-graph features. For these cases, we concatenate all these features for each node.

Inferring dynamic feature properties. To find dynamic feature properties, GNN-Infer first trains an interpretable model capturing the deviation between the actual GNN output and the specified output property P over the aggregated features. Then, GNN-Infer extracts the dynamic feature properties from these models. The actual type of model and how GNN-Infer uses the model depends on whether the GNN target a classification or a regression problem. For classification problems, GNN-Infer trains a decision tree capturing whether the output property P would hold with respect to the aggregated features. Next, GNN-Infer converts the paths of this decision tree that P holds into the corresponding dynamic feature predicates σ_{dyna} . GNN-Infer uses this predicate σ_{dyna} to extend the S_{LP} into dynamic properties S_{DP} taking the form $\sigma_{S \leq} \wedge \sigma_{dyna} \wedge \sigma_{inps} \Rightarrow P$. For regression problems, GNN-Infer trains a linear regression model over the aggregated features capturing the difference between the specified output P and the actual output of the GNN. GNN-Infer adds the regression model's term with the original output property to retrieve the extended output property P_{dyna} that can also capture these differences. In this case, the dynamic properties S_{DP} now takes the form $\sigma_{S \leq} \wedge \sigma_{inps} \Rightarrow P_{dyna}$.

In summary, the S_{DP} properties, which improve over S_{LP} , are defined as:

$$S_{DP} = \begin{cases} \sigma_{S \leq} \wedge \sigma_{inps} \wedge \sigma_{dyna} \Rightarrow P & \text{In classification problem} \\ \sigma_{S \leq} \wedge \sigma_{inps} \Rightarrow P_{dyna} & \text{In regression problem} \end{cases} \quad (5)$$

Example. For the GNN in Fig. 1, given the structure $S_1 = \langle \{1\}, \{\} \rangle$ containing only a single node 1, we show how GNN-Infer calculates the dynamic features and extends the following property $\sigma_{S_1 \leq} \wedge s_1 = 0 \Rightarrow s'_1 = 0$. First, GNN-Infer extracts the structural aggregated feature $x_1^{in} = \max(s_1) = s_1$ for node 1 since the structure contains only one node 1. GNN-Infer also extracts the full-graph aggregated feature for node 1 is $x_1^{full} = \max_{j \in \mathcal{N}(1)} s_j$. Thus, the set of dynamic features $f_{dyna_{S_1}}$ on S_1 will be: $f_{dyna_{S_1}} = (s_1, \max_{j \in \mathcal{N}(1)} s_j, \max_{j \in \mathcal{N}(1)} s_j - s_1)$

There are 4 matching instances of the input predicate of the property: the subgraphs containing a single node 0, 2, 3, 4 respectively in Fig. 3a. GNN-Infer calculates the corresponding $f_{dyna_{S_1}}$ for each of these nodes and obtains the following features (0, 1, 1), (0, 0, 0), (0, 1, 1), (0, 0, 0). Following this, GNN-Infer collects information on whether the property holds for each instance. The likely property holds on nodes 2, 4 and does not hold for nodes 0, 3. Using this information, GNN-Infer then trains a decision tree that predicts on which case the property holds. The learned decision tree on these features would result in the dynamic condition: $f_{dyna_{S_1}, 1} = 1 \Rightarrow holds$ where $f_{dyna_{S_1}, 1} = \max_{j \in \mathcal{N}(1)} s_j = 0$. Using the decision tree condition, the likely property would be transformed into the following dynamic feature property: $\sigma_{S_1 \leq} \wedge s_1 = 0 \wedge \max_{j \in \mathcal{N}(1)} (s_j) = 0 \Rightarrow s'_1 = 0$. This is the last output of GNN-Infer.

5 EVALUATION

GNN-Infer is written in ~20K lines of code in Python. We use Neo4j [34] for isomorphism checking, and PROPHECY[13] for inferring FNN properties. GNN-Infer takes as inputs a GNN produced using PyTorch [38], and the training dataset \mathcal{D} and outputs inferred properties of the GNN.

Below we evaluate the effectiveness of GNN-Infer in discovering GNN properties. We answer 3 research questions (RQs) as follows:

- **RQ1 (Correctness)** evaluates the quality of GNN-Infer’s resulting properties on both reference and trained GNNs;
- **RQ2 (Applications)** investigates the ability of GNN-Infer’s inferred properties on detecting backdoor attacks introduced by state-of-the-art methods on GNNs;
- **RQ3 (Efficiency)** measures the efficiency of GNN-Infer.

The experiment results reported here were obtained on an Intel i5-9600K machine with 6 cores at 3.7GHz clock speed and 64 GB of RAM running Linux.

5.1 Benchmarks

We evaluate GNNInfer on two benchmarks: (1) A benchmark of GNNs simulating classic algorithms and (2) a set of backdoored GNNs on two real-world datasets - Cora and Pubmed from [5].

GNNs simulating classic algorithms. To provide an initial thorough analysis of GNN-Infer’s correctness, we construct benchmarks of reference GNNs with identified correct properties and see if GNN-Infer can re-discover these known properties. Velickovic et al. [50] have shown that three classic graph algorithms, namely, Breadth-First search (BFS), Depth-First search (DFS), and Bellman-Ford shortest path (B-F), can be converted into message-passing networks with known properties.

All of these 3 tasks are node classification. Taking input as a graph with attributed nodes and edges, all 3 GNNs predict what are the next state (e.g., unvisited, under-visiting, or visited) of each node. The B-F GNN also predicts the next shortest distance from each node toward the original node (we use node 0 in all our experiments). We reuse these results to construct the reference GNNs and to check the correctness of GNN-Infer’s inferred properties. The number of ground-truth

Table 1. GNN benchmarks. Each target can have different types: classification (**C**) means GNN predicts discrete categories while regression (**R**) implies continuous predictions

Problem	Objective	Type	#L/#F	ltype	Avg. Perf.
BFS	Next state	C	1-3/2,4,8	mpnn, gcn	0.957
DFS	Next state	C	1-3/2,4,8	mpnn	1.0
	Next target	C	1-3/2,4,8	mpnn	0.978
B-F	Next state	C	1-3/2,4,8	mpnn	1
	Next distance	R	1-3/2,4,8	mpnn	$5.47e^{-4}$

properties for the reference GNN for BFS, DFS, and B-F are 3, 6, and 4 respectively. Details of these properties are explained in Appendix A.1.

We also create trained GNNs, which are learned automatically from the data generated by the original algorithm following the prior work [50]. Particularly, we implement 3 reference GNNs along with 33 trained GNNs created from widely used GNN layers i.e., MPNN [11] and GCN [25], for benchmark algorithms with various settings as shown in Tab. 1. The reference GNNs are correct while the other trained GNNs have varying performances as shown in the Appendix D, including Tabs. 5, 6 and 7.

Backdoored GNNs on real-world datasets. To further evaluate the capability of the inferred properties in defending and explaining backdoor behaviors, we employ backdoored GNNs created from the state-of-the-art backdoor attack method UGBA [5] on two real-world datasets: Cora [31] and Pubmed [43]. Out of three experimented GNNs chosen in UGBA, we experimented on Graph Convolution Networks (GCN) [25], GraphSAGE [14] as the Marabou verification tools [22] does not support quadratic operation in the graph attention layer of GAT. We use the same hyperparameters and training script from UGBA to obtain the trained GNNs.

5.2 RQ1. Correctness of GNN-Infer

We assess GNN-Infer’s effectiveness using known and trained GNNs (see Tab. 1). The "confidence score", or the likelihood of an inferred property holding for unseen data, is used to measure its performance. In classification tasks, this score is known as proxy accuracy (**PA**), representing the ratio of the output condition holding over satisfying inputs. For regression tasks, we use proxy error (**PE**), quantifying the deviation of the output condition from actual model predictions. Properties with **PA** > 0.9 or **PE** < 0.01 are deemed "likely-correct." We denote **PA** and **PE** before and after adding dynamic conditions (explained in Section 4.5) as **PA_{prior}**, **PA_{full}** and **PE_{prior}**, **PE_{full}** respectively. We quantify the dynamic conditions’ impact using the improvement rate (**IR**) of **PA** for classification and the reduction rate (**RR**) of **PE** for regression tasks. Detailed results for individual GNNs are in Appendix D with a summary provided below.

5.2.1 RQ1.1. How correct are the inferred properties on reference GNNs? We collect all the inferred properties for reference GNNs. Among the likely-correct properties, we further conducted a manual assessment to determine whether the inferred properties were equivalent to the desired properties. If the human annotators reached an agreement that a property is indeed equivalent to the desired properties, it was then marked as a **correct property**. The evaluation process involved two authors independently assessing the properties. If the two annotators disagreed on their decisions, a discussion will be conducted to reach a consensus.

Results. GNN-Infer inferred all 3 known properties for BFS. GNN-Infer inferred 2 out of 6 known properties for DFS. Additionally, GNN-Infer inferred 89 likely correct properties for DFS which approximate with the remaining 4 known properties of DFS. GNN-Infer discovered 3 out of the 4 known properties for B-F. Additionally, GNN-Infer inferred 5 likely properties for B-F that approximate the remaining one known property of B-F. None of the inferred properties on the reference GNNs has **PA** lower than 0.9. We give examples for each of these cases below.

Case studies. For BFS and B-F’s next state, the inferred properties correctly indicate 2 expected properties (1) if either there is a visited neighbor or the target node i itself is visited then it will be predicted as visited and (2) If all the surrounding neighbors and the target node i itself are unvisited, then its next state will also be unvisited as shown in the running example (see details in Section 3).

For B-F’s next distance, all the generated properties are likely correct with a very small deviation with respect to the ground-truth output conditions (less than 10^{-5}). For example, one of the inferred properties is: $\sigma_{S_0} \leq \wedge d_0 + w_{0,y} - d_y \geq 0 \Rightarrow d'_y = d_y - 0.99 f_{d_{yna}} + 4.29 \times 10^{-6}$ where $S_0 = \langle \{1, 0\}, \{(1, 0)\} \rangle$ and $f_{d_{yna}}$ is the offset between the minimum distances inside the structure and in the full input graph towards the target node 0. This shows that the new distance of node 0 is the minimum distance from all of its neighbors, with slight deviation due to the linear equation on the output being fit dynamically using features collected from the dataset.

For DFS, GNN-Infer captured properties describing when the next status of a node would either remain the same, enter an under-visiting state, and not be the next target. For example, in the structure $S_1 = \langle \{1\}, \{\} \rangle$ with one node 1, the properties $\sigma_{S_1} \leq \wedge s_{1,c} = 1 \wedge t_1 = 0 \Rightarrow s'_1 = c$ for $c \in \{0, 1, 2\}$ correctly described that if node 1 is not the visiting target, its state remains unchanged. For the next target objective, given a structure $S_3 = \langle \{0, 1, 2, 3\}, \{(0, 3), (1, 3), (2, 3)\} \rangle$ consisting of 4 nodes $\{0..3\}$ with node 3 being the target node with all other nodes having forward edges to and backward edges from node 3, GNN-Infer inferred the following property $s_{3,0} = 1 \wedge s_{3,1} = 1 \wedge t_3 = 1 \Rightarrow t'_3 = 0$, which correctly demonstrate that if node 3 currently is the target and has an under-visiting neighbor, it will not be the next target. GNN-Infer infers likely-correct properties when the ground truth condition involves quantifying terms such as there are no “unvisited” neighbors or the target node has the highest priority among another node’s neighbors. In these cases, GNN-Infer substitutes these conditions with the conditions of the target’s priority being higher or lower than a certain threshold, which is likely correct, but is not precise, on the whole dataset.

5.2.2 RQ1.2. How correct are the inferred properties on the trained GNNs and the contribution of dynamic analysis. To assess GNN-Infer’s performance on trained GNNs where we do not know the ground truth properties, we measure the confidence score (i.e., **PA** and **PE**) as well as the corresponding **IR** and **RR** on both the BFS, DFS, B-F GNNs and real-world GNNs from [5] in Tab. 2 and Tab. 3.

Results. GNN-Infer consistently delivered strong results with a **PA** of 0.95 (on a scale of 0-1.0) and a low average **PE** of 0.003 (over the maximum distance of 32 for B-F) across all tasks. On BFS and DFS Target tasks, GNN-Infer achieved high **PA** even prior to employing dynamic feature properties. For DFS state and B-F’s objectives, the introduction of dynamic properties led to **PA** improvements of 0.323, 0.356 and **PE** reduction of 0.999, demonstrating their effectiveness in capturing varying behaviors of B-F and DFS objectives.

Regarding the real-world GNNs in Tab 3, GNN-Infer achieved high **PA** (ranging from 0.7967 to 0.9982) and noticeable **IR** (up to 1.6453 on Cora for GCN), pointing to the potential benefits of dynamic conditions in enhancing generalization in real-world GNNs.

Table 2. Performance of GNN-Infer’s inferred properties on trained GNNs in BFS, DFS and B-F. Acc. is the accuracy of the models, MSE is the mean squared error of the model. PA is Proxy Accuracy, PE is the proxy error (MSE). IR is the proxy accuracy improvement rate and RR is the proxy error reduction rate

Method	Acc.		PA		IR	
	Mean	Std. dev	Mean	Std. dev	Mean	Std. dev
BFS State	0.953	0.106	0.977	0.045	0.083	0.055
DFS State	0.999	0.003	0.950	0.064	0.323	0.541
DFS Target	0.978	0.019	0.934	0.047	0.061	0.065
B-F State	1.000	0.000	0.970	0.046	0.356	0.224

Method	MSE		PE		RR	
	Mean	Std. dev	Mean	Std. dev	Mean	Std. dev
B-F Distance	0.001	0.001	0.003	0.004	0.999	0.001

Table 3. Performance of GNN-Infer’s inferred properties on real-world GNNs from UGBA [5]

Dataset	Model	Acc.	PA	IR	Model	Acc.	PA	IR
Cora	GCN	0.7812	0.9701	1.6453	GraphSage	0.7926	0.9905	0.095
Pubmed	GCN	0.8539	0.7967	0.4478	GraphSage	0.8523	0.9982	0.2403

RQ1: *GNN-Infer* consistently identified properties with high precision across all GNNs. For reference GNNs, manual assessment shows that, out of 13 ground truth properties, *GNN-Infer* inferred 8 correct properties and inferred likely properties that approximate the remaining properties. In trained GNNs, *GNN-Infer* demonstrated robust performance with an average **PA** of 0.95 and an average **PE** of 0.003. Notably, dynamic analysis contributed to a notable improvement in **PA** for the DFS state task by 32.3% and reduced the **PE** for the B-F distance task by 99.9%.

5.3 RQ2. Defending Against Backdoor Attacks

In this section, we show that *GNN-Infer* can be used to infer properties that help effectively defend against backdoor attacks of GNNs. We first provide a brief background on backdoor attacks on GNNs, and then explain how we use *GNN-Infer* to effectively defend against them.

Backdoor attacks on GNNs work in three phases: data poisoning, backdoor model training, and backdoored model requirement [5, 56, 63]. It is commonly assumed that the attacker can access and partially change the dataset of the trained model. This can be done via either publishing the poisoned dataset on an open-source platform, or exploiting the automated data collection process [7]. When other parties use the poisoned dataset to train a prediction model, this results in a backdoored model. When this backdoored model is deployed, the attackers can partially control this model by inserting a trigger. For example, in the sybil (fake user) detection problem [53], the attacker can manipulate few real users to like specific pages to increase the likelihood of users liking this page being real users. When the Sybil-detecting GNN is trained with this data, it may fail detecting fake users who liked the aforementioned page.

We aim at defending against such attack methods. We adopt a widely-used threat model, in which the developers of a GNN have access to both the training set and the clean test set, but do not know about which trigger is inserted, nor which sample is poisoned [5, 56, 63]. The task is to detect if the GNN is potentially planted with backdoors, and if so, identify the backdoored inputs and defend against them.

Backdoor attacks often follow three characteristics: stealthy, unnoticeable and effective [5, 56]. In detail, stealthy means that the backdoor behavior should not decrease the performance of the model on the test set. Unnoticeable means that the number of poisoned samples must be small and finally, effective means that the attack success rate (ASR) has to be high.

We propose to track the properties that warrant these characteristics by using a set of features that we explain below. Let $P := i_P \Rightarrow o_P$ be a property for a particular structure S , where $i_P := \sigma_{S \leq} \wedge \sigma_{inps} \wedge \sigma_{dyna}$ is the input condition and o_P is the output condition. It is important to note here again that $\sigma_{S \leq}$ is the subgraph isomorphism predicate. Let \mathcal{D}_{train} and \mathcal{D}_{test} be the training and testing set. Let $SP_{\mathcal{D}_{train}}^{i_P}$ and $SP_{\mathcal{D}_{test}}^{i_P}$ be the set of samples that satisfy the input condition i_P on the training set and the test set respectively. Furthermore, let $SP_{\mathcal{D}_{train}}^{\sigma_{S \leq}}$ and $SP_{\mathcal{D}_{test}}^{\sigma_{S \leq}}$ be the set of samples that satisfies the structure condition $\sigma_{S \leq}$ on the training and test set as well. Finally, let $SP_{\mathcal{D}_{train}}^{o_P}$, $SP_{\mathcal{D}_{test}}^{o_P}$ be the set of samples that satisfy the output condition o_P on the training and test set. We show that the backdoor behaviors can be modeled using these features. To model unnoticeability, meaning that the number of poisoned samples has to be sufficiently small, we hypothesize that the properties that model the behaviors of these poisoned samples would have a small number of supporting samples in the training data as well. We define the support rate as $SPR_{\mathcal{D}_{train}}^{i_P} = |SP_{\mathcal{D}_{train}}^{i_P}| / |SP_{\mathcal{D}_{train}}^{\sigma_{S \leq}}|$. We choose this rate to be 0.1 for a property to be unnoticeable. There may be concerns that being unnoticeable does not mean the property represents a backdoor. Thus, we further strengthen backdoor properties by also modeling stealthiness and effectiveness. Recall that stealthiness means the backdoored model has to perform well on the test set. For the poisoned model to perform well on the test set, there must be much fewer test samples that support the backdoor behavior than on the training set. We model this behavior by identifying properties that have significantly higher support rate on the training set than on the test set: $SPR_{\mathcal{D}_{test}}^{i_P} / SPR_{\mathcal{D}_{train}}^{i_P} < \tau_S$ where τ_S is a chosen threshold (we set this to 0.05). We call the properties that match stealthiness and unnoticeability likely-backdoor properties. Likely backdoor properties are considered as backdoor properties once they model the ‘‘effectiveness’’ characteristic. We model the effectiveness by checking the overriding rate: between a likely backdoor property P_{likely} and a ‘‘benign’’ (i.e., unlikely to be backdoor properties) property P_{benign} , the overriding rate (OR) is defined as the number of samples that model the input conditions in both P_{likely} and P_{benign} , but

the prediction only satisfy the output condition of P_{likely} : $OR_{P_{likely}}^{P_{benign}} = \frac{|SP_{\mathcal{D}_{train}}^{i_{P_{likely}} \wedge i_{P_{benign}} \wedge o_{P_{likely}}}|}{|SP_{\mathcal{D}_{train}}^{i_{P_{likely}} \wedge i_{P_{benign}}}|}$

Recall that the structure condition specifies whether the graph contains a subgraph. Since a graph can contain multiple substructures, a single node can also match multiple input conditions of different properties. In these cases, if the backdoor properties are effective, their output condition should override the other properties. We choose the likely properties that have a mean overriding rate towards the benign properties $\geq 80\%$ to be the backdoor properties. After identifying all these backdoor properties, we prune the edges of subgraphs that match these backdoor properties.

We compare the defensive performance of GNN-Infer versus two state-of-the-art baselines proposed in [4, 5, 69], Prune and Prune+LD. Prune discards edges based on the similarity between the target node and the neighboring nodes’ hidden features and Prune+LD additionally discards (isolate) the labels of the nodes of the discarded edges. These homophily-based baselines are widely used in literature [4, 69] for defending against graph backdoors, but have limitations in detecting backdoors planted by UGBA [5], which we aim to improve.

Results. The result is presented in Tab. 4. GNN-Infer consistently outperforms Prune and Prune+LD on both datasets. Particularly, on the Cora dataset and GCN architecture, the success

Table 4. Performance of different defensive methods towards UGBA. **ACC** is the accuracy of the trained GNN on the clean dataset, **ASR** is the original attack success rate without any defensive method. For GNN-Infer, Prune, and Prune-LD, the **D-ACC** is the accuracy of the trained GNN after the defensive method is added and **D-ASR** is the attack success rate after the defensive method is applied.

Model	Dataset	ACC	ASR	Prune		Prune+LD		GNN-Infer	
				D-ACC	D-ASR	D-ACC	D-ASR	D-ACC	D-ASR
GCN	Cora	0.781	0.996	0.782	0.991	0.781	0.993	0.774	0.834
GraphSage	Cora	0.793	0.996	0.794	0.981	0.796	0.985	0.770	0.959
GCN	Pubmed	0.851	0.972	0.854	0.973	0.841	0.951	0.852	0.914
GraphSage	Pubmed	0.852	0.942	0.851	0.929	0.853	0.931	0.854	0.893

reduction rate of GNN-Infer is 16.2%, outperforming Prune (0.5%) and Prune LD (0.3%) by more than 30 times. On Cora and with GraphSage, GNN-Infer reduced the attack success rate by 3.7% in comparison with 1.5% and 1.1% of Prune and Prune+LD respectively. On the Pubmed dataset, GNN-Infer reduced the attack success rate by 5.8% on GCN and 4.9% on GraphSage in comparison with 2.1% and 1.1% of Prune+LD and 0.0% and 1.3% of Prune. While the coverage of the inferred properties can be limited, leading to limitations in identifying and pruning all backdoor properties, we note that, after performing the pruning, the accuracies of the GNNs on the clean test node on all cases only deviated from the original accuracy by 0.023 at maximum. This shows that the inferred properties are capable of precisely isolating the backdoor behaviors.

RQ2: *GNN-Infer's* performance in precisely identifying and neutralizing backdoor properties of backdoored GNN without affecting the clean accuracy is promising. In detail, GNN-Infer outperformed existing baselines by a significant margin: achieving a success reduction rate on the Cora dataset with the GCN architecture that was more than 30-fold higher than the baseline methods (16.2% vs. 0.5%/0.3%) while does not affect the clean test accuracy by more than 0.023 from the original clean test accuracy.

5.4 RQ3. Efficiency of GNN-Infer

We measure the performance of GNN-Infer across its three described stages: structure extraction, structure-specific analysis, and dynamic analysis. Since each stage depends on the size of the input graph and the total number of input graphs, we measure the performance of GNN-Infer with respect to the data volume. Specifically, we choose the benchmark-representative sample size of 1000, as seen in widely recognized dataset like Cora [31] and Pubmed [5, 43]. We describe the performance of GNN-Infer in each stage below.

Structural Extraction. This stage consists of performing explanation by GNNExplainer [61], followed by performing mining with gSpan [57]. We measured the total runtime across the experimenting datasets and obtained an average runtime of 2 hours. Most of this runtime is occupied by GNNExplainer (which takes approximately 2 hours). Mining takes only from 10-20 seconds on all datasets. The runtime of GNNExplainer is mostly dedicated to optimizing a mask on each sample and on each prediction GNN, which takes around 7 – 8 seconds per graph.

Structure-specific Analysis. This stage consists of graph matching of influential structures, converting GNN into FNN, running instrumentation, and inferring properties based on the obtained execution traces. This stage takes another 2 hours on our settings. While the GNN-to-FNN conversion is very efficient (taking up only less than 1 second), performing graph matching and property

inference are less efficient. We note that 1,000 input graphs can contain several hundred thousand instances. For our evaluation, in which the maximum number of retrieved instances was set at 100,000, this retrieval takes up to 20 minutes. In terms of property inference, since iterative relaxation of properties requires verification, this takes up to 90 minutes.

Dynamic Analysis. Dynamic analysis only concerns the first layer of GNN, so run time is nearly constant given the number of samples. In our case, this takes less than 90 seconds for all properties.

Backdoor defense. After inferring properties, we can optionally include a backdoor defense stage (see Section 5.3). The backdoor defense consists of identifying the backdoor properties and performing pruning of these properties. The backdoor properties identification takes 2 minutes in our settings for each test set and for each structure, given that we obtained the training support set from the structure-specific analysis stage. Since pruning requires performing graph-isomorphism checking again and pruning the structure having matched features, it takes up to 30 minutes for the largest structure containing 3 nodes and 7 edges. In our experiments, this takes a total of 2 hours.

RQ3: The inference process of GNN-Infer takes approximately 4 hours in total as upper bound in our experiment. While GNN-to-FNN conversion is very efficient (takes less than one second), other steps such as explanation, graph matching, and property inference are less efficient. While there is room to improve efficiency, we believe that the current efficiency of GNN-Infer is reasonable for offline processing.

6 DISCUSSION

In this section, we discuss how GNN-Infer can be used for debugging GNN models given certain expected properties, enabling a property-based approach to GNN debugging.

To demonstrate this idea, we conduct a small analysis of the three problems - BFS, DFS, and B-F and show how the inferred properties can be used in conjunction with the expected properties to debug GNN models. Firstly, if GNN-Infer infers high-confident properties that follow the desired property, the developers can be more confident that the analyzed GNN is correct. As an example, the following inferred properties with high confidence score on dfs_1 in Section 5.2: $\sigma_{S_1 \leq} \wedge s_{1,0} = 1 \wedge t_1 = 0 \Rightarrow s'_1 = 0$, shows that this GNN is likely to model well the property that if a node is unvisited and it is not the target, it will stay unvisited. Secondly, if GNN-Infer discovers a property having high confidence score but contradicts an expected property, then these properties can help highlight the GNNs' error. For instance, consider the GNN bfs_1 in Tab. 5. We see a property $\sigma_{S_0 \leq} \wedge s_1 = 0 \wedge s_0 = 1 \Rightarrow s'_0 = 0$ with a perfect confidence score, but is wrong with respect to the expected behavior: bfs_1 incorrectly predicts a node as unvisited even if it is already visited, given the presence of an unvisited neighbor. Finally, we can also identify GNNs' error by finding the properties that agree with the ground truth but having low confidence scores, such as two inferred properties of bfs_5 from Tab. 5: (i) $\sigma_{S_1 \approx} \wedge s_1 = 0 \wedge \max_{j \in \mathcal{N}(1)} s_j = 0 \Rightarrow s'_1 = 0$, and (ii) $\sigma_{S_0 \leq} \wedge s_1 = 0 \wedge s_0 = 1 \Rightarrow s'_0 = 1$. These properties together suggest that the GNN probably fails in modeling the case where the node and its surrounding neighbors are all unvisited, or the transition from unvisited to visited of one node.

These analyses hint that it is possible to use inferred properties to ensure GNN's correctness as well as highlight its errors if we are given expected properties. Since most of the current machine

learning problems do not come with expected properties, an interesting future direction would be applying GNN-Infer to different models to infer a set of common expected properties that every future-developed model should have.

7 RELATED WORK

Neural Network Analysis. The line of work that is closely related to GNN-Infer is inferring properties [10, 13, 35], verification of properties [8, 20, 21, 23] and repairing networks with properties [12, 46, 49] for DNN. PROPHECY [13] proposed the usage of using activation patterns of ReLU [1] and max-pool [26] to infer DNN’s properties in the form of an input condition implying an output condition, both in the form of linear inequalities. [10] proposed a mining-based approach using activation patterns to infer DNN properties and apply them as neural network specifications. Both [10, 13] can only infer FNN and CNN properties and cannot be applied to infer GNN properties, which GNN-Infer aims to address. GNN-Infer’s method to debug GNN also differs from existing property-based DNN debugging works [12, 46, 49]. These works try searching for the weights that let the DNN model a set of expected properties. They ensure the correctness of the new weights using the DNN verification techniques [8, 9, 20–23, 33, 45, 54]. Since the used verification techniques have yet to support GNNs due to the same varying structure problem, these debugging techniques [12, 46, 49] cannot be applied on GNNs either. GNN-Infer instead uses the inferred properties as filters to remove backdoored input. Finally, we note that GNN-Infer is the first fully developed, implemented, and thoroughly evaluated tool that analyzes GNNs through FNN conversion. Recent work [35] gives an outline of ideas about GNN analysis via FNN. However, it only provides sketch ideas without any algorithms, formal analyses, implementations, applications on backdoor defense, or evaluations.

Backdoor attacks on Graph Neural Networks. Backdoor attacks against deep learning model in general is a specific type of data poisoning. Backdoor attacks work in two phases: the data collection phase and the training phase. In the data collection phase, the attacker poisons the training dataset by attaching triggers to a set of samples with target labels. Training the model on this dataset would result in a backdoored model that associates the presence of the trigger to the target label. This gives the attacker partial control over the model’s output. SBA [63] initiates backdoor attacks on GNN by attaching a fixed graph to every poisoned sample. GTA [56] adopts an adaptive trigger generation via bi-level optimization and UGBA further increases the efficiency of backdoor attack by efficiently choosing representative nodes to attach the trigger. While SBA and GTA’s attack can be defended by using the homophily property graph neural networks, namely, with Prune and Prune+LD in [5], none of these methods are effective against UGBA. Our framework can also be seen as a tool to analyze and defend against backdoor attacks, by detecting the properties that match the backdoor characteristics, we can defend against these properties by removing subgraphs that model these properties. CARE [46] also tries applying particle swarm optimization to adjust neural network weights to defend against backdoor attacks. However, CARE requires to know the poisoned samples beforehand, which might not be practical. On the other hand, GNN-Infer infers the backdoor properties automatically without these restrictions.

Explaining Graph Neural Networks. Our work can also be regarded as a different way to aid understanding GNNs. In this line of work, [60] introduced a method using meta-gradient to optimize a mask of the important score for each node, edge, and feature, [40] proposes encoding the problem of identifying important features using an SMT formulation and solves it using SMT solver, [19] proposes a framework to compute the most significant features and [52] explains GNN by inferring a probabilistic graphical model and PGExplainer [28] learns a model predicting the important score of each node and edge. While these works aim to directly attribute which part of the input is

responsible for the output to help human experts gain intuition to debug the GNNs, GNN-Infer outputs properties. These properties can represent a class of correctness or faulty inputs as seen in Section 6. Since PGM Explainer [52] also outputs a probabilistic graphical model that can be regarded as a probabilistic formula relating the input and output of the model, it would be interesting to see additional work built upon PGM Explainer for automated debugging of GNNs in future works.

8 CONCLUSION AND FUTURE WORK

We introduced GNN-Infer, a property inference tool for GNN. The foundation of GNN-Infer is the formal proof and the algorithm to reduce a graph neural network with a specific structure into an equivalent FNN. Based on this, GNN-Infer infers the GNN’s property on the given specific structure by using property inference tool on the reduced FNN. Finally, GNN-Infer generalizes the inferred structure-specific properties to a class of input graph that contain the chosen structure with dynamic analysis. Experiment results demonstrated that GNN-Infer can infer correct and highly confident properties on both synthetic as well as real-world GNNs. Furthermore, we also used GNN-Infer’s inferred properties to detect and defend against the state-of-the-art backdoor attack, namely UGBA [5]. Experiments showed that GNN-Infer increases the defense rate up to 30 times in comparison with the two defense baselines. For future works, we plan to improve GNN-Infer and use it for other tasks, e.g., verification of GNNs.

REFERENCES

- [1] Abien Fred Agarap. 2018. Deep Learning using Rectified Linear Units (ReLU). <https://doi.org/10.48550/ARXIV.1803.08375>
- [2] Miltiadis Allamanis, Marc Brockschmidt, and Mahmoud Khademi. 2018. Learning to Represent Programs with Graphs. In *International Conference on Learning Representations*.
- [3] Quentin Cappart, Didier Chételat, Elias B. Khalil, Andrea Lodi, Christopher Morris, and Petar Veličković. 2021. Combinatorial Optimization and Reasoning with Graph Neural Networks. In *Proceedings of the Thirtieth International Joint Conference on Artificial Intelligence, IJCAI-21*, Zhi-Hua Zhou (Ed.). International Joint Conferences on Artificial Intelligence Organization, 4348–4355. Survey Track.
- [4] Yongqiang Chen, Han Yang, Yonggang Zhang, Kaili Ma, Tongliang Liu, Bo Han, and James Cheng. 2022. Understanding and Improving Graph Injection Attack by Promoting Unnoticeability. In *International Conference on Learning Representations*. <https://openreview.net/forum?id=wkMG8cdvh7->
- [5] Enyan Dai, Minhua Lin, Xiang Zhang, and Suhang Wang. 2023. Unnoticeable Backdoor Attacks on Graph Neural Networks. In *Proceedings of the ACM Web Conference 2023*. 2263–2273.
- [6] Hanjun Dai, Hui Li, Tian Tian, Xin Huang, Lin Wang, Jun Zhu, and Le Song. 2018. Adversarial attack on graph structured data. In *International conference on machine learning*. PMLR, 1115–1124.
- [7] Ruyi Ding, Shijin Duan, Xiaolin Xu, and Yunsi Fei. 2023. VertexSerum: Poisoning Graph Neural Networks for Link Inference. <https://doi.org/10.48550/ARXIV.2308.01469>
- [8] Ruediger Ehlers. 2017. Formal verification of piece-wise linear feed-forward neural networks. In *International Symposium on Automated Technology for Verification and Analysis*. Springer, 269–286.
- [9] Timon Gehr, Matthew Mirman, Dana Drachler-Cohen, Petar Tsankov, Swarat Chaudhuri, and Martin Vechev. 2018. AI2: Safety and Robustness Certification of Neural Networks with Abstract Interpretation. In *2018 IEEE Symposium on Security and Privacy (SP)*. IEEE, 3–18. <https://doi.org/10.1109/SP.2018.00058>
- [10] Chuqin Geng, Nham Le, Xiaojie Xu, Zhaoyue Wang, Arie Gurfinkel, and Xujie Si. 2023. Towards Reliable Neural Specifications. In *International Conference on Machine Learning*. PMLR, 11196–11212.
- [11] Justin Gilmer, Samuel S Schoenholz, Patrick F Riley, Oriol Vinyals, and George E Dahl. 2017. Neural message passing for quantum chemistry. (2017), 1263–1272.
- [12] Ben Goldberger, Guy Katz, Yossi Adi, and Joseph Keshet. 2020. Minimal Modifications of Deep Neural Networks using Verification. In *LPAR23. LPAR-23: 23rd International Conference on Logic for Programming, Artificial Intelligence and Reasoning (EPiC Series in Computing, Vol. 73)*, Elvira Albert and Laura Kovacs (Eds.). EasyChair, 260–278. <https://doi.org/10.29007/699q>
- [13] Divya Gopinath, Hayes Converse, Corina S. Pasareanu, and Ankur Taly. 2019. Property Inference For Deep Neural Networks. *2019 34th IEEE/ACM International Conference on Automated Software Engineering (ASE)* (4 2019), 797–809.

- [14] William L. Hamilton, Rex Ying, and Jure Leskovec. 2017. Inductive Representation Learning on Large Graphs. In *Proceedings of the 31st International Conference on Neural Information Processing Systems* (Long Beach, California, USA) (NIPS'17). Curran Associates Inc., Red Hook, NY, USA, 1025–1035.
- [15] Kaiming He, Xiangyu Zhang, Shaoqing Ren, and Jian Sun. 2016. Deep Residual Learning for Image Recognition. *2016 IEEE Conference on Computer Vision and Pattern Recognition (CVPR)*, 770–778. <https://doi.org/10.1109/CVPR.2016.90>
- [16] Kaiming He, Xiangyu Zhang, Shaoqing Ren, and Jian Sun. 2016. Identity mappings in deep residual networks. *Lecture Notes in Computer Science (including subseries Lecture Notes in Artificial Intelligence and Lecture Notes in Bioinformatics)* 9908 LNCS (2016), 630–645.
- [17] Xing Hu, Ge Li, Xin Xia, David Lo, and Zhi Jin. 2018. Deep code comment generation. In *2018 IEEE/ACM 26th International Conference on Program Comprehension (ICPC)*. IEEE, 200–20010.
- [18] Qiang Huang, Makoto Yamada, Yuan Tian, Dinesh Singh, and Yi Chang. 2023. GraphLIME: Local Interpretable Model Explanations for Graph Neural Networks. *IEEE Transactions on Knowledge and Data Engineering* 35, 7 (2023), 6968–6972. <https://doi.org/10.1109/TKDE.2022.3187455>
- [19] Qiang Huang, Makoto Yamada, Yuan Tian, Dinesh Singh, Dawei Yin, and Yi Chang. 2020. GraphLIME: Local Interpretable Model Explanations for Graph Neural Networks. (1 2020). <http://arxiv.org/abs/2001.06216>
- [20] Xiaowei Huang, Marta Kwiatkowska, Sen Wang, and Min Wu. 2017. Safety verification of deep neural networks. In *International conference on computer aided verification*. Springer, 3–29.
- [21] Guy Katz, Clark Barrett, David L Dill, Kyle Julian, and Mykel J Kochenderfer. 2017. Reluplex: An efficient SMT solver for verifying deep neural networks. In *International Conference on Computer Aided Verification*. Springer, 97–117.
- [22] Guy Katz, Derek A Huang, Duligur Ibeling, Kyle Julian, Christopher Lazarus, Rachel Lim, Parth Shah, Shantanu Thakoor, Haoze Wu, Aleksandar Zeljić, et al. 2019. The marabou framework for verification and analysis of deep neural networks. In *International Conference on Computer Aided Verification*. Springer, 443–452.
- [23] Guy Katz, Derek A. Huang, Duligur Ibeling, Kyle Julian, Christopher Lazarus, Rachel Lim, Parth Shah, Shantanu Thakoor, Haoze Wu, Aleksandar Zeljić, David L. Dill, Mykel J. Kochenderfer, and Clark Barrett. 2019. The Marabou Framework for Verification and Analysis of Deep Neural Networks. *Lecture Notes in Computer Science (including subseries Lecture Notes in Artificial Intelligence and Lecture Notes in Bioinformatics)* 11561 LNCS (2019), 443–452.
- [24] Nikhil S. Ketkar, Lawrence B. Holder, and Diane J. Cook. 2005. Subdue: Compression-based frequent pattern discovery in graph data. *Proceedings of the ACM SIGKDD International Conference on Knowledge Discovery and Data Mining* January (2005), 71–76.
- [25] Thomas N. Kipf and Max Welling. 2016. Semi-Supervised Classification with Graph Convolutional Networks. (9 2016).
- [26] Alex Krizhevsky, Ilya Sutskever, and Geoffrey E. Hinton. 2012. ImageNet Classification with Deep Convolutional Neural Network. *Proceedings of the 25th International Conference on Neural Information Processing Systems* 1 (2012), 1097–1105.
- [27] Weibo Liu, Zidong Wang, Xiaohui Liu, Nianyin Zeng, Yurong Liu, and Fuad E Alsaadi. 2017. A survey of deep neural network architectures and their applications. *Neurocomputing* 234 (2017), 11–26.
- [28] Dongsheng Luo, Wei Cheng, Dongkuan Xu, Wenchao Yu, Bo Zong, Haifeng Chen, and Xiang Zhang. 2020. Parameterized Explainer for Graph Neural Network. *Advances in Neural Information Processing Systems* 33 (2020).
- [29] Jiaqi Ma, Junwei Deng, and Qiaozhu Mei. 2022. Adversarial Attack on Graph Neural Networks as An Influence Maximization Problem. In *Proceedings of the Fifteenth ACM International Conference on Web Search and Data Mining* (Virtual Event, AZ, USA) (WSDM '22). Association for Computing Machinery, New York, NY, USA, 675–685. <https://doi.org/10.1145/3488560.3498497>
- [30] Jiaqi Ma, Shuangrui Ding, and Qiaozhu Mei. 2020. Towards more practical adversarial attacks on graph neural networks. *Advances in neural information processing systems* 33 (2020), 4756–4766.
- [31] Andrew Kachites McCallum, Kamal Nigam, Jason Rennie, and Kristie Seymore. 2000. *Information Retrieval* 3, 2 (2000), 127–163. <https://doi.org/10.1023/a:1009953814988>
- [32] Dimitrios Michail, Nikos Kanakaris, and Iraklis Varlamis. 2022. Detection of fake news campaigns using graph convolutional networks. *International Journal of Information Management Data Insights* 2, 2 (2022), 100104. <https://doi.org/10.1016/j.jjimei.2022.100104>
- [33] Christoph Müller, François Serre, Gagandeep Singh, Markus Püschel, and Martin Vechev. 2020. Scaling Polyhedral Neural Network Verification on GPUs. (7 2020).
- [34] Neo4j. 2017. The Neo4j Developer Manual v3.3.
- [35] Thanh-Dat Nguyen, Thanh Le-Cong, ThanhVu Le, Nguyen H., Xuan Bach D, and Quyet Thang Huynh. 2022. Towards the Analysis of Graph Neural Network. In *ACM/IEEE 44nd International Conference on Software Engineering: New Ideas and Emerging Results* (Pittsburgh, USA) (ICSE '22). Association for Computing Machinery.
- [36] Thanh-Dat Nguyen, Thanh Le-Cong, Duc-Minh Luong, Van-Hai Duong, Xuan-Bach D Le, David Lo, and Quyet-Thang Huynh. 2022. FFL: Fine-grained Fault Localization for Student Programs via Syntactic and Semantic Reasoning. *The 38th IEEE International Conference on Software Maintenance and Evolution* (11 2022).

- [37] Daniel W Otter, Julian R Medina, and Jugal K Kalita. 2020. A survey of the usages of deep learning for natural language processing. *IEEE transactions on neural networks and learning systems* 32, 2 (2020), 604–624.
- [38] Adam Paszke, Sam Gross, Francisco Massa, Adam Lerer, James Bradbury, Gregory Chanan, Trevor Killeen, Zeming Lin, Natalia Gimelshein, Luca Antiga, Alban Desmaison, Andreas Kopf, Edward Yang, Zachary DeVito, Martin Raison, Alykhan Tejani, Sasank Chilamkurthy, Benoit Steiner, Lu Fang, Junjie Bai, and Soumith Chintala. 2019. PyTorch: An Imperative Style, High-Performance Deep Learning Library. In *Advances in Neural Information Processing Systems* 32. Curran Associates, Inc., 8024–8035. <http://papers.neurips.cc/paper/9015-pytorch-an-imperative-style-high-performance-deep-learning-library.pdf>
- [39] Michael Pradel and Satish Chandra. 2021. Neural software analysis. *Commun. ACM* 65, 1 (2021), 86–96.
- [40] Subham Sekhar Sahoo, Subhashini Venugopalan, Li Li, Rishabh Singh, and Patrick Riley. 2020. Scaling Symbolic Methods using Gradients for Neural Model Explanation. (6 2020).
- [41] Franco Scarselli, Marco Gori, Ah Chung Tsoi, Markus Hagenbuchner, and Gabriele Monfardini. 2008. The graph neural network model. *IEEE transactions on neural networks* 20, 1 (2008), 61–80.
- [42] Michael Schlichtkrull, Thomas N. Kipf, Peter Bloem, Rianne van den Berg, Ivan Titov, and Max Welling. 2017. Modeling Relational Data with Graph Convolutional Networks. (2017).
- [43] Prithviraj Sen, Galileo Namata, Mustafa Bilgic, Lise Getoor, Brian Gallagher, and Tina Eliassi-Rad. 2008. Collective Classification in Network Data. *AI Magazine* 29, 3 (Sep. 2008), 93. <https://doi.org/10.1609/aimag.v29i3.2157>
- [44] Sanjit A Seshia, Ankush Desai, Tommaso Dreossi, Daniel Fremont Shromona, Ghosh Edward Kim, Sumukh Shivakumar, Marcell Vazquez-Chanlatte, Xiangyu Yue, and Daniel J Fremont Shromona. 2018. Formal Specification for Deep Neural Networks. <http://www2.eecs.berkeley.edu/Pubs/TechRpts/2018/EECS-2018-25.html>
- [45] Gagandeep Singh, Timon Gehr, Markus Püschel, and Martin Vechev. 2019. An abstract domain for certifying neural networks. *Proceedings of the ACM on Programming Languages* 3 (1 2019). Issue POPL. <https://doi.org/10.1145/3290354>
- [46] Bing Sun, Jun Sun, Long H. Pham, and Jie Shi. 2022. Causality-Based Neural Network Repair. In *Proceedings of the 44th International Conference on Software Engineering (Pittsburgh, Pennsylvania) (ICSE '22)*. Association for Computing Machinery, New York, NY, USA, 338–349. <https://doi.org/10.1145/3510003.3510080>
- [47] Yue Sun, Zhi Yang, and Yafei Dai. 2020. TrustGCN: Enabling Graph Convolutional Network for Robust Sybil Detection in OSNs. In *2020 IEEE/ACM International Conference on Advances in Social Networks Analysis and Mining (ASONAM)*. 1–7. <https://doi.org/10.1109/ASONAM49781.2020.9381325>
- [48] Qiaoyu Tan, Ninghao Liu, Xing Zhao, Hongxia Yang, Jingren Zhou, and Xia Hu. 2020. Learning to hash with graph neural networks for recommender systems. In *Proceedings of The Web Conference 2020*. 1988–1998.
- [49] Muhammad Usman, Divya Gopinath, Youcheng Sun, Yannic Noller, and Corina S. Păsăreanu. 2021. NNrepair: Constraint-Based Repair Of Neural Network Classifiers. In *Computer Aided Verification: 33rd International Conference, CAV 2021, Virtual Event, July 20–23, 2021, Proceedings, Part I*. Springer-Verlag, Berlin, Heidelberg, 3–25. https://doi.org/10.1007/978-3-030-81685-8_1
- [50] Petar Veličković, Rex Ying, Matilde Padovano, Raia Hadsell, and Charles Blundell. 2019. Neural execution of graph algorithms. *arXiv* (2019).
- [51] Athanasios Voulodimos, Nikolaos Doulamis, Anastasios Doulamis, and Eftychios Protopapadakis. 2018. Deep learning for computer vision: A brief review. *Computational intelligence and neuroscience* 2018 (2018).
- [52] Minh N. Vu and My T. Thai. 2020. PGM-explainer: Probabilistic graphical model explanations for graph neural networks. *arXiv* (2020). Issue NeurIPS.
- [53] Binghui Wang, Le Zhang, and Neil Zhenqiang Gong. 2017. SybilSCAR: Sybil detection in online social networks via local rule based propagation. In *IEEE INFOCOM 2017 - IEEE Conference on Computer Communications*. 1–9. <https://doi.org/10.1109/INFOCOM.2017.8057066>
- [54] Shiqi Wang, Kexin Pei, Justin Whitehouse, Junfeng Yang, and Suman Jana. 2018. Formal security analysis of neural networks using symbolic intervals. In *27th USENIX Security Symposium (USENIX Security 18)*. 1599–1614.
- [55] Huijun Wu, Chen Wang, Yuriy Tyshetskiy, Andrew Docherty, Kai Lu, and Liming Zhu. 2019. Adversarial Examples for Graph Data: Deep Insights into Attack and Defense. In *Proceedings of the Twenty-Eighth International Joint Conference on Artificial Intelligence, IJCAI-19*. International Joint Conferences on Artificial Intelligence Organization, 4816–4823.
- [56] Zhaohan Xi, Ren Pang, Shouling Ji, and Ting Wang. 2021. Graph Backdoor. In *30th USENIX Security Symposium (USENIX Security 21)*. USENIX Association, 1523–1540. <https://www.usenix.org/conference/usenixsecurity21/presentation/xi>
- [57] Xifeng Yan and Jiawei Han. 2002. gspan: Graph-based substructure pattern mining. In *2002 IEEE International Conference on Data Mining, 2002. Proceedings*. IEEE, 721–724.
- [58] Xinli Yang, David Lo, Xin Xia, Yun Zhang, and Jianling Sun. 2015. Deep learning for just-in-time defect prediction. In *2015 IEEE International Conference on Software Quality, Reliability and Security*. IEEE, 17–26.
- [59] Rex Ying, Ruining He, Kaifeng Chen, Pong Eksombatchai, William L Hamilton, and Jure Leskovec. 2018. Graph convolutional neural networks for web-scale recommender systems. In *Proceedings of the 24th ACM SIGKDD International Conference on Knowledge Discovery & Data Mining*. 974–983.

- [60] Zhitao Ying, Dylan Bourgeois, Jiaxuan You, Marinka Zitnik, and Jure Leskovec. 2019. Gnnexplainer: Generating explanations for graph neural networks. *Advances in neural information processing systems* 32 (2019).
- [61] Zhitao Ying, Dylan Bourgeois, Jiaxuan You, Marinka Zitnik, and Jure Leskovec. 2019. GNNExplainer: Generating Explanations for Graph Neural Networks. In *Advances in Neural Information Processing Systems*, Vol. 32. Curran Associates, Inc.
- [62] Tom Young, Devamanyu Hazarika, Soujanya Poria, and Erik Cambria. 2018. Recent trends in deep learning based natural language processing. *IEEE Computational Intelligence Magazine* 13, 3 (2018), 55–75.
- [63] Zaixi Zhang, Jinyuan Jia, Binghui Wang, and Neil Zhenqiang Gong. 2021. Backdoor Attacks to Graph Neural Networks. In *Proceedings of the 26th ACM Symposium on Access Control Models and Technologies*. ACM. <https://doi.org/10.1145/3450569.3463560>
- [64] Jianan Zhao, Xiao Wang, Chuan Shi, Binbin Hu, Guojie Song, and Yanfang Ye. 2021. Heterogeneous Graph Structure Learning for Graph Neural Networks. *Aaai* (2021).
- [65] Jie Zhou, Ganqu Cui, Shengding Hu, Zhengyan Zhang, Cheng Yang, Zhiyuan Liu, Lifeng Wang, Changcheng Li, and Maosong Sun. 2020. Graph neural networks: A review of methods and applications. , 57-81 pages. <https://doi.org/10.1016/j.aiopen.2021.01.001>
- [66] Yaqin Zhou, Shangqing Liu, Jingkai Siow, Xiaoning Du, and Yang Liu. 2019. Devign: Effective vulnerability identification by learning comprehensive program semantics via graph neural networks. *Advances in neural information processing systems* 32 (2019).
- [67] Yu Zhou, Haixia Zheng, Xin Huang, Shufeng Hao, Dengao Li, and Jumin Zhao. 2022. Graph Neural Networks: Taxonomy, Advances, and Trends. *ACM Trans. Intell. Syst. Technol.* 13, 1, Article 15 (jan 2022), 54 pages. <https://doi.org/10.1145/3495161>
- [68] Dingyuan Zhu, Ziwei Zhang, Peng Cui, and Wenwu Zhu. 2019. Robust graph convolutional networks against adversarial attacks. In *Proceedings of the 25th ACM SIGKDD International Conference on Knowledge Discovery & Data Mining*. 1399–1407.
- [69] Xu Zou, Qinkai Zheng, Yuxiao Dong, Xinyu Guan, Evgeny Kharlamov, Jialiang Lu, and Jie Tang. 2021. TDGIA: Effective Injection Attacks on Graph Neural Networks. In *Proceedings of the 27th ACM SIGKDD Conference on Knowledge Discovery and Data Mining (Virtual Event, Singapore) (KDD '21)*. Association for Computing Machinery, New York, NY, USA, 2461–2471. <https://doi.org/10.1145/3447548.3467314>
- [70] Daniel Zügner and Stephan Günnemann. 2019. Adversarial Attacks on Graph Neural Networks via Meta Learning. In *International Conference on Learning Representations*. <https://openreview.net/forum?id=Bylnx209YX>

A APPENDIX

A.1 Detailed Problem Settings

A.1.1 BFS. The BFS GNN takes as input a graph in which each node i has a state feature s_i , $s_i = 0$ if this node is unvisited and $s_i = 1$ if this node is visited. Given that a set of node is initially visited, this GNN would predict the state of each node in the next visiting iteration.

Groundtruth property As stated in [50], it is desired that GNNs follow the following properties:

- (1) If a node i is visited, then it will continue to be *visited*: $s_i = 1 \Rightarrow s'_i = 1$
- (2) If a node i has a visited neighbor j , in the next step, it will be visited $\exists j$ s.t. $(j, i) \in E \wedge s_j = 1 \Rightarrow s'_i = 1$.
- (3) If both i and its surrounding neighbors are unvisited, then it will continue to be unvisited $\forall j \in \mathcal{N}(i), s_j = 0 \wedge s_i = 0 \Rightarrow s'_i = 0$.

Reference GNN We design a GNN model which is guaranteed to behave according to the desired properties. Particularly, we construct the reference GNN for the Parallel BFS problem based on [50], taking as input a graph $G = (V_G, E_G)$

$$m_{j,i} = f_{msg}(s_j, s_i) = s_j \quad (6)$$

$$\bar{m}_i = f_{agg}(m_{j,i} | (j, i) \in E_G) = \max_{j \in \mathcal{N}(i)} m_{j,i} \quad (7)$$

$$s'_i = f_{upd}(\bar{m}_i, s_i) = \bar{m}_i \quad (8)$$

This would result in $y_i = \max_{j \in \mathcal{N}(i) \cup \{i\}} s_j$. This relation between the input s_j

A.1.2 DFS. The DFS GNN takes as input also a graph, with each node i having two features $\begin{pmatrix} s_i \\ t_i \end{pmatrix}$. $s_i = 0$ if the node is unvisited, 1 if undervisiting and 2 if visited. The additional feature t_i is used to determine which exact node is underwriting. At each step, the DFS would predict (1) which node to be undervisiting next t'_i and the next state s'_i of all nodes. The next undervisiting node will have feature $t'_i = 1$, while the rest have $t'_i = 0$. To describe DFS as a message passing procedure, we present the algorithm for 2 objectives in Fig. 6, Fig. 7.

Algorithm We describe in detail the algorithm for each objective *next state* and *next visiting target* in Algorithm 6 and Algorithm 7, respectively.

```

input : Target node  $t$ , States map  $S$ , node  $i$ 
output: The new state  $s'_i$  for node  $i$ 
1 if  $i \neq t$  then return  $S[i]$ 
2 Unvisited neighbors set  $U_{i,f} \leftarrow \{j \in \mathcal{N}_f(i) | S[j] = 0\}$ 
3 if  $U_{i,f} \neq \emptyset$  then return 1
4 else return 2
    
```

Fig. 6. Determine the next state for node i

input : Target node t , States map S , priority function P , Target node next state s'_i
output : Next visiting target node nt

```

1 if  $s'_i = 1$  then
2   | return  $\arg \min_{j \in \mathcal{N}_f(t) | S[j]=0} P(j)$ 
3 else
4   | under-visiting node set  $V_t \leftarrow \{j \in \mathcal{N}_b(t) | S[j] = 1 \wedge j \neq t\}$ 
5   | if  $V_t = \emptyset$  then
6   |   | return -1
7   | return  $\arg \max_{j \in V_t} P(j)$ 
    
```

Fig. 7. Determine the next visiting target

Where $\mathcal{N}_f(i)$ and $\mathcal{N}_b(i)$ identify all the forwards and backwards neighbors of node i respectively, finally, given the new target node nt , the edge from the current target node t to nt will be added to the *backward* edge: $E_G = E_G \cup \{(nt, t)\}$, $\lambda_G = \lambda_G \cup \{(nt, t) \mapsto 1\}$. Note that the GNN only makes two predictions on node-level and the input graph's edges are already added in the dataset at each step.

Ground truth property With respect to the next state output:

- If the node is not the target, then the output class should be the same: $t_i = 0 \wedge s_{i,0} = 1 \Rightarrow s'_i = 0$, $t_i = 0 \wedge s_{i,1} = 1 \Rightarrow s'_i = 1$, $t_i = 0 \wedge s_{i,2} = 1 \Rightarrow s'_i = 2$.
- If the node is the target, then if there exists a forward *unvisited* neighbor, the next state will be *under-visiting* $t_i = 1 \wedge (\max_{j \in \mathcal{N}_f(i)} s_{j,0}) = 1 \Rightarrow s'_i = 1$
- Otherwise, next state will be *visited* $t_i = 1 \wedge (\max_{j \in \mathcal{N}_f(i)} s_{j,0} = 0) \Rightarrow s'_i = 2$

With respect to the next target determination:

- If the node is the target, then it will not be the next target $t_i = 0 \Rightarrow t'_i = 0$
- If the node is the target's smallest priority *unvisited* forward neighbor, then it will be the next target. $s_{i,0} = 1 \wedge t_i = 0 \exists j \in \mathcal{N}_b(i) \wedge t_j = 1 \wedge p_i = \min_{i' \in \mathcal{N}_f(j)} p_{i'} \Rightarrow t_i = 1$
- If the node is the target's largest priority *under-visiting* backward neighbor, and the target node does not have any forward *visited* neighborhood, then it will be the next target. $s_{i,1} = 1 \wedge t_i = 0 \exists j \in \mathcal{N}_f(i) \wedge t_j = 1 \wedge p_i = \max_{i' \in \mathcal{N}_b(j)} p_{i'} \wedge \max_{i' \in \mathcal{N}_f(j)} s_{i',0} = 0 \Rightarrow t_i = 1$

Correct Reference GNN

$$s'_i = \begin{cases} s_i & \text{if } t_i = 0 \\ 1 & \text{if } t_i = 1 \wedge \max_{j \in \mathcal{N}(i) \setminus \{i\}} s_{j,0} = 1 \\ 2 & \text{otherwise} \end{cases} \quad (9)$$

To derive the message passing form of s'_i , we split the calculation of its values into 3 cases: $s'_{i,0}$, $s'_{i,1}$, $s'_{i,2}$ corresponding to node i next state to be predicted as *unvisited*, *undervisiting* and *visited*. s'_i 's value is determined by $s'_i = \arg \max_j s'_{i,j}$ and given C is a large number (we choose 100 in our implementation).

- $s'_{i,0} = \text{ReLU}(-Ct_i + s_{i,0})$ If node i is not the target node, the value of $s'_{i,0}$ will be 0, otherwise, it will be the former value $s_{i,0}$.
- $s'_{i,1} = \text{ReLU}\left(-C\left((1-t_i) + \min_{j \in \mathcal{N}_f(i)} (1-s_{j,0} + t_j)\right) + 1\right) + \text{ReLU}(-Ct_i + s_{i,1})$. If node i is the target node (i.e., $t_i = 1$, then the first term will be reduced to the indication of whether there exists a node j different from node i such that node j current state is *visited*. Otherwise, if $t_i = 0$, $s'_{i,1}$ will be reduced to $s_{i,1}$
- $s'_{i,2} = 1 - s'_{i,0} - s'_{i,1}$

The min terms in $s'_{i,1}$ can be straight-forwardly implemented using the message passing mechanism, for example, for $s'_{i,1}$:

$$m_{j \rightarrow i} = \text{ReLU}(1 - s_{j,0} + t_j) \quad (10)$$

$$\bar{m}_i = \min_{j \in \mathcal{N}_f(i)} m_{j,i} \quad (11)$$

$$s'_{i,1} = \text{ReLU}(-C((1 - t_i) + \bar{m}_i)) + 1 + \text{ReLU}(-Ct_i + s_{i,1}) \quad (12)$$

The next target node objective is rather challenging since GNNs infer node-level classification has to infer the result based solely on the node's updated hidden feature (i.e., the next target node has to know that it is the highest-priority forward *visited* neighbor of a target node or the highest-priority backward *under-visiting* neighbor.)

Since the GNN compute node's next hidden features based solely on the current neighbor's feature, we use a message passing mechanism to save the aforementioned top-priority forward unvisited (*tfu*) neighbor and top-priority backward undervisiting (*tbu*) neighbor and another message passing procedure so that corresponding neighbor acknowledges that it is the next target node.

For any node i , the *lfu* can be calculated using the following equation:

$$lfu_i = \text{ReLU}(\max_{j \in \mathcal{N}_f(i)} (p_j - C(1 - s_{j,0} + t_j))) \quad (13)$$

$$lbu_i = \text{ReLU}(\max_{j \in \mathcal{N}_b(i)} (p_j - C(1 - s_{j,1} + t_j))) - C \cdot lfu_i \quad (14)$$

lfu_i and lbu_i is equal to the maximum priority of the node i 's forward *visited* and backward *undervisiting* neighbors respectively. The term t_j ensures that j is not the current target node.

$$t'_i = \begin{pmatrix} \text{ReLU} \max_{j \in \mathcal{N}_b(i)} \left(\begin{array}{l} 1 - \\ C(1 - t_j + \text{ReLU}(lfu_j - p_i)) + \\ \text{ReLU}(p_i - lfu_j) - C \cdot t_i \end{array} \right) + \\ \text{ReLU} \max_{j \in \mathcal{N}_f(i)} \left(\begin{array}{l} 1 - \\ C(1 - t_j + \text{ReLU}(lbu_j - p_i)) + \\ \text{ReLU}(p_i - lbu_j) \end{array} \right) - \\ C \cdot t_i \end{pmatrix} \quad (15)$$

A.1.3 Bellman-Ford. Bellman-Ford (B-F) GNN takes as input a graph where each node is assigned with feature $x_i = \begin{pmatrix} s_i \\ d_i \end{pmatrix}$ where $s_i \in \{0, 1\}$ is the current state of the node (visited or unvisited) and d_i is the current shortest distance from the node to the root node (node 0) and each edge is associated with a weight feature w_{ji} , denoting the weight of the edge $(j, i) \in E$.

Ground truth property There exists 2 ground-truth properties regarding the node i 's next updated distance and also its visited state. Regarding node i 's visited state:

- (1) If all the surrounding node of i is *visited* and node i is also *visited* then node i will be marked as *visited*: $s_i = 0 \wedge \max_{j \in \mathcal{N}(i)} s_j = 0 \Rightarrow s'_i = 0$. The structure predicate, in this case, consists of a node i , and its out-of-structure neighbors' features $\max_{j \in \mathcal{N}(i)}$.
- (2) If node i is *visited*, then it will continue to be predicted as *visited*: $s_i = 1 \Rightarrow s'_i = 1$. In this case, the structure predicate only consists of a single node i .
- (3) If there exists a node j in the node i 's neighbor such that node j state is *visited*, then node i will be marked as *visited* $\max_{j \in \mathcal{N}(i)} s_j = 1 \Rightarrow s'_i = 1$. In this case, the structure predicate consists of a node i and a node j which the state is *visited*.

Regarding node i new distance: node i 's updated distance is the minimum between its current distance and the sum of each neighbor j 's distance and weight toward i : $d'_i = \min(\min_{j \in \mathcal{N}(i)} d_j +$

$w_{j,i}, d_i$). The structure predicate may consist of 1 node when its new distance remains the same and 2 nodes or when the new distance is updated.

Reference GNN The reference GNN is straightforward, comprising of 2 message passing operations: the reused message passing operation from Parallel BFS and the following message passing operation for calculating d'_i . Given that the GNN add self-loops (which is a common setting in the implementation of GNN) for each node:

$$m_{j,i} = d_j + w_{j,i} \quad (16)$$

$$\bar{m}_i = \min_{j \in \mathcal{N}(i)} m_{j,i} \quad (17)$$

$$d'_i = \bar{m}_i \quad (18)$$

$$(19)$$

B REDUCTION

We give detailed proof of each lemma and theorem below.

PROOF. (Lemma 1) Let $L_i^{(k)}$ be the k th layer of \mathcal{M}_i , $V_i^{(l)}$ and $V_{i+1}^{(l)}$ be $L_i^{(k)}$'s input and output variable sets, respectively. Let $U^{(k)} = \bigcup_{i=1}^n V_i^{(k)}$ be the union of output variable sets $V_i^{(k)}$ with $1 \leq i \leq n$ and n_k be the number of elements of $U^{(k)}$.

Consider the relation $L^{(k)}$ between $U^{(k-1)}$ and $U^{(k)}$ are combination of k^{th} layers of every neural network $\mathcal{M}_1, \dots, \mathcal{M}_n$ with $1 \leq k \leq l$:

$$L^{(k)}(x_1^{(k-1)}, \dots, x_{n_{k-1}}^{(k-1)}) = (x_1^{(k)}, \dots, x_{n_k}^{(k)}) \quad (20)$$

where, $x_1^{(j)}, \dots, x_{n_j}^{(j)}$ are all of distinct variables in $U^{(j)}$.

We can prove that each relation is actually a function by proving each valuation of $(x_1^{(k-1)}, \dots, x_{n_{k-1}}^{(k-1)})$ are assigned to one and only one valuation of $(x_1^{(k)}, \dots, x_{n_k}^{(k)})$.

Indeed, let us assume that there exists a two valuation of $(x_1^{(k)}, \dots, x_{n_k}^{(k)})$: $(v(x_1^{(k)}), \dots, v(x_{n_k}^{(k)}))$ and $(v'(x_1^{(k)}), \dots, v'(x_{n_k}^{(k)}))$ such that:

$$L^{(k)}(v(x_1^{(k-1)}), \dots, v(x_{n_{k-1}}^{(k-1)})) = (v(x_1^{(k)}), \dots, v(x_{n_k}^{(k)})) \quad (21)$$

$$L^{(k)}(v(x_1^{(k-1)}), \dots, v(x_{n_{k-1}}^{(k-1)})) = (v'(x_1^{(k)}), \dots, v'(x_{n_k}^{(k)})) \quad (22)$$

$$(v(x_1^{(k)}), \dots, v(x_{n_k}^{(k)})) \neq (v'(x_1^{(k)}), \dots, v'(x_{n_k}^{(k)})) \quad (23)$$

Equation 23 implies that there exists at least one variable $x_*^{(k)}$ of $U^{(k)}$:

$$v(x_*^{(k)}) \neq v'(x_*^{(k)}) \quad (24)$$

Without loss of generality, we can assume that $x_*^{(k)}$ is $x_1^{(k)}$. Since $\mathcal{M}_1, \dots, \mathcal{M}_n$ are different, meaning that their variable sets $V_1^{(k)}, \dots, V_n^{(k)}$ are distinct. This implies that $x_1^{(k)}$ belongs to one and only one variable set $V_*^{(k)}$ of layer $L_*^{(k)}$ of neural network \mathcal{M}_* .

We also have the input variable set of $L_*^{(k)}$ is a subset of $U^{(k-1)}$. Without loss of generality, we suppose that $x_1^{(k-1)}, \dots, x_{|V_*^{(k-1)}|}^{(k-1)}$ ($|V_*^{(k-1)}|$ is the number of elements of $V_*^{(k-1)}$) are all of the input variables of $L_*^{(k)}$. We have:

$$v(x_1^{(k)}) = L_*^{(k)}(v(x_1^{(k-1)}), \dots, v(x_{|V_*^{(k-1)}|}^{(k-1)})) \quad (25)$$

$$v'(x_1^{(k)}) = L_*^{(k)}(v(x_1^{(k-1)}), \dots, v(x_{|V_*^{(k-1)}|}^{(k-1)})) \quad (26)$$

From Equation 24, 25 and 26, we can see that $L_*^{(k)}$ can output different values with the same input and thus a contradiction because $L_*^{(k)}$ is a function.

Thus, we now can conclude that $L^{(k)}$ is a function.

Moreover, as $L^{(k)}$ is a combination of $L_1^{(k)}, \dots, L_m^{(k)}$, $L^{(k)}$ is one of the following: (1) affine transformation, (2) the RELU activation function (3) a max pooling function.

Therefore, following Definition 2, we can conclude that the combination of $\mathcal{M}_1, \dots, \mathcal{M}_n$, which is a composition of L functions $L^{(1)}, \dots, L^{(l)}$ is a feed-forward neural network (Q.E.D). \square

PROOF. (Lemma 2) Suppose that \mathcal{M}_i is the composition of l_i layers:

$$\begin{aligned} L_i^{(1)} &: \mathbb{R}^{n_i} \rightarrow \mathbb{R}^{n_i} \\ &\dots \\ L_i^{(l_i)} &: \mathbb{R}^{n_{i-1}} \rightarrow \mathbb{R}^{n_{i+1}} \end{aligned}$$

Then, we have the composition $\mathcal{M}_1, \dots, \mathcal{M}_k$ is the composition of $\sum_{i=0}^k l_i$ layer as follows: li

$$\begin{aligned} L_1^{(1)} &: \mathbb{R}^{n_1} \rightarrow \mathbb{R}^{n_1} \\ &\dots \\ L_1^{(l_1)} &: \mathbb{R}^{n_{i-1}} \rightarrow \mathbb{R}^{n_2} \\ &\dots \\ L_k^{(1)} &: \mathbb{R}^{n_k} \rightarrow \mathbb{R}^{n_k} \\ &\dots \\ L_k^{(l_k)} &: \mathbb{R}^{n_{k-1}} \rightarrow \mathbb{R}^{n_{k+1}} \end{aligned}$$

, where each layer $L_i^{(j)}$ is a feedforward layer in Def. 1

Therefore, we can conclude that the composition $\mathcal{M}_1, \dots, \mathcal{M}_k$ is also a feed-forward neural network following Definition 2 (Q.E.D). \square

PROOF. (Lemma 3) Since the result of a GNN layer is produced by

$$\mathbf{x}'_i = f_{upd}(\mathbf{x}_i, f_{agg}(\{f_{msg}(\mathbf{x}_j, \mathbf{x}_i, \mathbf{e}_{ji}) \mid (j, i) \in E\}))$$

Since the hidden features $\mathbf{x}_i \in \mathbb{R}^D$ is constructed by an FNN and f_{msg} is an FNN, each $f_{msg}(\mathbf{x}_j, \mathbf{x}_i, \mathbf{e}_{ji})$ is also an FNN by Lemma 2. Furthermore, since E remains unchanged, f_{agg} is mean, max, or sum aggregation of these individual FNN is also an FNN. In detail, since E is fixed, the number of incoming edges towards any node i remains unchanged. Thus, every choice of f_{agg} will lead to an FNN layer:

- If f_{agg} is mean aggregation, with a fixed number of elements, this reduces to a linear combination of its elements, with each coefficient set to a fixed value of inversed number of incoming edges.
- If f_{agg} is max aggregation, with a fixed number of elements, this reduces to a fixed-size max pooling.
- If f_{agg} is sum aggregation, with a fixed number of elements, this reduces to a linear combination of its elements with coefficients set to 1.

Thus, since f_{agg} becomes an FNN layer that composites multiple other FNN layers as input (i.e., each f_{msg}), this part of a GNN layer is also an FNN. Finally, f_{upd} is already FNN according to 2, and the GNN layer is reduced to an FNN (Q.E.D). \square

Finally, we show that by recursively applying these reductions, a GNN is converted to an equivalent FNN in Theorem 1

PROOF. (Theorem 1) **Base Case:** We consider a GNN \mathcal{M} with a single message-passing layer, as defined by Definition 3. According to Lemma 3, such a GNN layer can be reduced to an FNN layer because the operations of message passing can be emulated by appropriate weight matrices and non-linear function in an FNN. Thus for a GNN with a single layer, the theorem holds as the GNN is equivalent to an FNN.

Inductive Hypothesis: Assume that for a GNN \mathcal{M} with k layers, where $k \geq 1$, the computation of the first k layers is equivalent to an FNN \mathcal{M}_{F_k} . This is our inductive hypothesis, which asserts that for k layers, the computation on any graph structure S can be performed by an equivalent FNN.

Inductive Step: Now, consider a GNN \mathcal{M} with $k+1$ layers. By inductive hypothesis, the computation of the first k layers of \mathcal{M} can be performed by an FNN \mathcal{M}_{F_k} . For the $(k+1)$ -th layer of \mathcal{M} , by Lemma 3, this layer can also be reduced to an FNN layer. By Lemma 2, the composition of this additional layer with the previously obtained FNN \mathcal{M}_{F_k} yields another FNN, which we will denote as $\mathcal{M}_{F_{k+1}}$. Hence, the first k layers combined with the $(k+1)$ -th layer form an FNN equivalent to the original GNN with $k+1$ layers.

Conclusion Having shown that the addition of each layer in a GNN can be mirrored by a corresponding layer in an equivalent FNN, we conclude that for a GNN \mathcal{M} with any number of layers, this procedure reduces \mathcal{M} to an equivalent FNN \mathcal{M}_F that computes the same function on any given fixed graph structure S . Therefore, Theorem 1 is proven. \square

C TRANSFORMATION AS REWRITING RULES

Previously, we have shown that given a fixed structure (i.e., fixed edge set E). By reducing a f_{agg} of the first layer, a GNN is reducible to an FNN in a bottom-up manner. Let us formalize these transformations as rewriting rules.

In detail, let's assume the fixed structure has the edge set E with node set V . The input to GNN is now variable node feature matrix $\mathbf{X} \in \mathbb{R}^{|V| \times D_V}$ and edge feature matrix $\mathbf{E} \in \mathbb{R}^{|E| \times D_E}$. We can further enforce an ordered edge set E by introducing a comparison operator between 2 edge: $(i_1, j_1) < (i_2, j_2) \Leftrightarrow i_1 < i_2$ or $i_1 = i_2 \wedge j_1 < j_2$. And let $idx(j, i)$ be the function that map from two nodes (j, i) to the edge index in this order. Recall that the set of all messages passing between all edges in E is calculatable by $f_{msg}(\mathbf{x}_j, \mathbf{x}_i, \mathbf{e}_{ij}) \forall (j, i) \in E$.

$$\frac{idx(j, i) \mapsto idx_e}{f_{msg}(\mathbf{x}_j, \mathbf{x}_i, \mathbf{e}_{ij}) \forall (j, i) \in E \rightarrow f_{msg}(\mathbf{X}_{E_{idx_e,0,:}}, \mathbf{X}_{E_{idx_e,1,:}}, \mathbf{E}_{idx_e})} \quad (27)$$

This has a meaningful implication: since the matrix-row selection is representable as a linear transformation, given the index function, we can now batch calculate all message with only linear operation. Astute readers might notice that this is analogous to the adjacency matrix-based representation of GNN in [25]. This is indeed a correct observation, however, we keep this annotation to keep precise semantic towards message passing networks [11], which is a more general representation. We can also calculate the index of incoming edges for each node i : $InIdx : i \mapsto \{idx(j, i) | (j, i) \in E\}$. Thus, for each node i , the aggregation can be rewritten as:

$$\frac{InIdx(i) \mapsto IID_e}{f_{agg}(\{f_{msg}(\mathbf{x}_j, \mathbf{x}_i, \mathbf{e}_{ji}) \forall j | (j, i) \in E\}) \rightarrow f_{agg}(f_{msg}(\mathbf{X}_{E_{IID_e,0,:}}, \mathbf{X}_{E_{IID_e,1,:}}, \mathbf{E}_{IID_e}))} \quad (28)$$

This f_{agg} aggregates over a *fixed-dimension* matrix by the result of f_{msg} , thus, it is further reducible based on the actual chosen aggregation function:

$$\text{mean} (f_{msg}(\mathbf{X}_{E_{IID_e,0,:}}, \mathbf{X}_{E_{IID_e,1,:}}, \mathbf{E}_{IID_e})) \rightarrow \frac{1}{|IID_e|} f_{msg}(\mathbf{X}_{E_{IID_e,0,:}}, \mathbf{X}_{E_{IID_e,1,:}}, \mathbf{E}_{IID_e}) \quad (29)$$

$$\text{max} (f_{msg}(\mathbf{X}_{E_{IID_e,0,:}}, \mathbf{X}_{E_{IID_e,1,:}}, \mathbf{E}_{IID_e})) \rightarrow \max (f_{msg}(\mathbf{X}_{E_{IID_e,0,:}}, \mathbf{X}_{E_{IID_e,1,:}}, \mathbf{E}_{IID_e})) \quad (30)$$

$$\text{sum} (f_{msg}(\mathbf{X}_{E_{IID_e,0,:}}, \mathbf{X}_{E_{IID_e,1,:}}, \mathbf{E}_{IID_e})) \rightarrow [1, 1, \dots, 1]^T (f_{msg}(\mathbf{X}_{E_{IID_e,0,:}}, \mathbf{X}_{E_{IID_e,1,:}}, \mathbf{E}_{IID_e})) \quad (31)$$

Finally, the update would remain the same but takes input as transformed f_{msg} and f_{agg} instead. This results in an FNN layer. By recursively applying these transformations, according to Theorem 1’s proof. We obtain an FNN.

Example. For the case of S_0 , $\mathbf{X} = \begin{pmatrix} s_0 \\ s_1 \end{pmatrix} \in \mathbb{R}^{2 \times 1}$, and there would be no edge feature matrix \mathbf{E} .

For the other example such as bellman-ford in [50] where edge weight is needed, each edge feature matrix’s row can store a single edge weight. In the aforementioned example of BFS, the set of message would be from node 1 to node 0, node 0 to node 0 and node 1 to node 1. Since it has 3 edges $\{(1, 0), (0, 0), (1, 1)\}$, for node 0, $\text{InIdx}(0) = \{0, 1\}$ and $\text{InIdx}(1) = \{1\}$ for node 1. We elaborate the process of transforming index selection to linear transformation as below. We construct incoming edge selection for node 0, $E_{s,0} = \begin{pmatrix} 1 & 0 \\ 0 & 1 \end{pmatrix}$ (first row selecting the index 0 and 2nd row selecting the index 1). The message for node 0 according to this selection matrix is:

$$f_{msg} \left(\mathbf{X} \cdot E_{s,0}, \mathbf{X} \begin{bmatrix} 1 & 0 \\ 1 & 0 \end{bmatrix} \right) = \begin{bmatrix} s_1 \\ s_0 \end{bmatrix} \quad (32)$$

The aggregated message for node 0 would be transformed into: $\max(s_1, s_0)$. The same process is repeated for s_1 . Finally, transforming the update function would give us the final FNN:

$$\text{NS} = \mathbf{X}^{(1)} = \bar{\mathbf{M}} = \begin{pmatrix} \max(s_0, s_1) \\ s_1 \end{pmatrix} \quad (33)$$

D DETAILS OF BENCHMARK

Tabs. 5, 6, and 7 shows the performance of individual GNNs and the respective proxy score of GNN-Infer. Each of the three tables provides details about GNNs trained on BFS, DFS, and B-F problems. Columns #L and #F indicate the number of layers and hidden features in each layer, respectively, while **ltype** denotes the types of layers used, such as neural message passing or graph convolution, particularly for the BFS problem Fig. 1.

BFS GNNs delivered robust results, except for bfs_1 and bfs_2 , with accuracy ranging from 0.9 to 1.0. DFS GNNs scored near-perfect accuracy for the *next state* objective and high-performance (≥ 0.95) for the *next visiting target* objective. B-F GNNs exhibited decent performance, with GNN-Infer’s properties achieving a proxy MSE below 0.012 for the next distance objective and a proxy accuracy from 0.89 for the next state objective.

GNN-Infer’s properties achieved perfect proxy accuracy for 15 GNNs and displayed high-confidence proxy accuracy from 0.888 to 0.918 for the remaining 4 GNNs. However, perfect proxy scores were only achieved for dfs_5 in *next state* and dfs_1 in *next target*.

GNN-Infer’s properties showed high proxy scores for both objectives, ranging from 0.93 for 8 GNNs to 0.79 for dfs_8 in *next state*, and from 0.8799 for the *next visiting target* objective.

Looking at the **IR** values across tables 5, 6, and 7, we see that for most cases in BFS and DFS’s next state and DFS’s next visiting target, the addition of dynamic predicates leads to an improvement of

Table 5. Performance of 17 trained GNN for BFS.

Name	#L/#F	ltype	SA	PA	IR
ref	1/1	mpnn	1	1	0.115
bfs ₁	1/2	gcn	0.73	1	0.053
bfs ₂	1/2	gcn	1	1	0.144
bfs ₃	1/4	gcn	1	1	0.144
bfs ₄	2/2	gcn	0.63	1	0
bfs ₅	2/4	gcn	0.90	0.888	0.0042
bfs ₆	2/8	gcn	0.90	0.888	0.0033
bfs ₇	3/2	gcn	1	1	0.115
bfs ₈	3/4	gcn	1	0.89	0.0011
bfs ₉	3/8	gcn	1	1	0.115
bfs ₁₀	1/2	mpnn	1	1	0.115
bfs ₁₁	1/4	mpnn	1	1	0.115
bfs ₁₂	2/2	mpnn	1	1	0.115
bfs ₁₃	2/4	mpnn	1	1	0.115
bfs ₁₄	2/8	mpnn	1	1	0.115
bfs ₁₅	3/2	mpnn	1	0.918	0.0026
bfs ₁₆	3/4	mpnn	1	1	0.115
bfs ₁₇	3/8	mpnn	1	1	0.115

less than 20%. This indicates that the structure-specific properties can largely model the GNNs’ behaviors even without dynamic predicates, but these dynamic features still play a role in enhancing the precision of the properties. For certain cases like dfs_8 where structure-specific properties fail to adequately capture GNN behavior, the dynamic analysis can provide the necessary conditions for the property to hold in the full graph. This is seen in sections Section 5.2 and Section 5.3.

Interestingly, dynamic analysis drastically reduces proxy MSE for B-F’s next distance by factors between 10^3 to 10^6 . Moreover, the improvement of B-F’s next state objective is significantly higher than its BFS counterpart despite having the same reference GNN.

Overall, dynamic analysis can boost the accuracy of the final properties for most cases and in some cases, it can even be the main contributor to the property’s precision in modeling the behavior of GNNs. In summary, the inferred properties demonstrate strong proxy measures across all three problems, indicating GNN-Infer’s capability to identify properties that effectively represent the GNNs’ behaviors in both classification and regression tasks. It’s important to note that there are instances where the model performance is less robust yet the proxy accuracy remains highly confident. Conversely, there are also cases of perfect model performance accompanied by less-than-perfect proxy accuracy, which we have discussed in Section 6.

Table 6. Performance of 8 trained GNNs and reference GNN accuracy for DFS.

Name	#L/#F	Next State			Next Visiting Target		
		SA	SPA	SIR	TA	TPA	TIR
ref	2/2	1	0.931	0.084	1	0.880	0.150
dfs ₁	1/2	1	0.955	0.402	0.950	1	0
dfs ₂	1/4	1	0.955	0.010	0.964	0.959	0.009
dfs ₃	2/2	1	0.956	0.026	0.961	0.963	0.001
dfs ₄	2/4	1	0.972	0.164	0.988	0.889	0.167
dfs ₅	2/8	1	1	0	0.995	0.889	0.061
dfs ₆	3/2	0.990	0.994	0.551	0.960	0.993	0.004
dfs ₇	3/4	1	0.993	0	0.988	0.931	0.091
dfs ₈	3/8	1	0.791	1.667	0.996	0.899	0.064

Table 7. Performance of 8 trained GNNs and reference GNN accuracy for B-F.

Name	#L/#F	Next Distance			Next State		
		DE	DPE	DIR	SA	SPA	SIR
ref	1/2	0.0	$2e^{-9}$	1	1	1	0.145
blmfd ₁	1/2	$1.4e^{-4}$	$1.04e^{-3}$	0.996	1	1	0.364
blmfd ₂	1/4	$1.2e^{-4}$	$5.21e^{-3}$	0.999	1	0.927	0.162
blmfd ₃	2/2	$3e^{-3}$	$8.32e^{-3}$	0.998	1	0.891	$5.5e^{-4}$
blmfd ₄	2/4	$1e^{-3}$	$5.2e^{-4}$	1	1	1	0.325
blmfd ₅	2/8	$1.9e^{-4}$	$2.3e^{-4}$	1	1	1	0.42
blmfd ₆	3/2	$1.8e^{-4}$	$3.01e^{-3}$	0.999	1	0.911	0.697
blmfd ₇	3/4	$1.23e^{-4}$	$7.93e^{-7}$	1	1	1	0.551
blmfd ₈	3/8	$1.7e^{-4}$	$1.15e^{-2}$	0.999	1	1	0.535